NAM

Special Report on the
Loppersum earthquakes – December 2017

Datum December 2017

Editors Taco den Bezemer and Jan van Elk

Contents

1 Summary

Two additional earthquakes in the Loppersum area contributed to an exceedance of a Measurement and Control Protocol (MRP) parameter (Earthquake density) at the signalling level. The same two earthquakes also caused the MRP activity rate to be exceeded at the alertness level. Both the earthquake density and the activity rate have been fluctuating in the past couple of months around the signalling level and the alertness level respectively after an increase in both parameters early this year. This report is written in accordance with the MRP, and is used to support a decision on whether new control measures are required given the current seismicity development.

This report starts by outlining the general status of all MRP parameters on December 10th and analyses the situation around 't Zandt in some depth. It is shown in this report that no other MRP parameters are exceeded and that there are no unexpected seismicity developments (e.g. no anomalies in PGA and PGV or seismicity developing in unexpected places) but that the general trend of earthquakes in the Loppersum area needs to be watched, as also concluded in reports earlier this year. The context of the earthquake density exceedance is sketched using seismicity trends in the area. It is argued in this report that the exceedance of earthquake density did not result from changing subsurface conditions but is the product of the general increase in seismicity in the Loppersum area already concluded in an earlier report. To further assess the context of this earthquake density exceedance, a question also addressed in this report is whether fluctuations and trends in earthquake density can be expected without any change in subsurface conditions; it is shown that it is indeed possible to exceed threshold values without an underlying worsening of seismicity conditions.

The analysis in this report proceeds with an analysis of the two recent 't Zandt earthquakes. The first observation is that the hypocentres of the earthquakes plot on two different faults with rather limited off-set. The next observation is that the last 't Zandt earthquake associates somewhat (in time) with a (relative) production peak in the cluster of 't Zandt. Subsequent pressure analysis, however, shows little further obvious correlations, unless the derivative of pressure is used. Further work is suggested and outlined based on analysis of individual faults with the ultimate aim of addressing the question of whether particular faults in the area need specific attention for seismicity development.

The report concludes that the most obvious additional production measure is to review the production operations procedure for getting rid of liquids in the production pipework and judge its merits against a potentially slightly increased risk of triggering (small) earthquakes. It is also argued that no other new control measures are yet required; no new area has become seismically active and our modelling (2 independent models) suggest a stabilisation of the number of earthquakes for the next couple of years. Moreover, and probably more importantly, the expected "earthquake reducing effect" of the recently taken production measure (10% overall volume reduction, from 24 mrd m^3 average per year to 21.6 mrd m^3 per year) that has become effective per the 1st of October 2017, may take some 6 to 9 months to show its effect.

2 Introduction

Two earthquakes occurred close to the ‘t Zandt village in the municipality of Loppersum in early December 2017. The first event occurred on 6th December at 23:28:59 (UTC) and the second on 10th December at 16:48:33, with M_L magnitudes reported by KNMI as 1.8 and 2.1, respectively. These earthquakes contributed to an exceedance of the MRP parameter earthquake density at the signalling level (see reference 1 for explanation of the structure and rationale of MRP). These same earthquakes also caused another MRP parameter (Activity Rate) to be exceeded at the alertness level (waakzaamheidsniveau).

This recent development fits in a context of a somewhat increased level of seismicity in the Loppersum area as extensively discussed in reference 2 (Periodical Report on Groningen Seismicity). In this report, it was concluded that the seismicity increase in the Loppersum area is statistically significant and needs to be watched. This report also presented two forecasts (from 2 different models) for the Loppersum area, which showed that this increase in seismicity is not expected to continue for the next 5 years but is likely to fluctuate as a function of random variations. This report should be read in conjunction with reference 1 as they are complementary.

This report is basically structured in four parts. The first part (Sections 3-7) sketch the status of the MRP parameters. The second part analyses the earthquakes around ‘t Zandt in some depth. The third part analyses some trends and investigates some patterns in parameters that are thought to be correlated with seismicity development. The fourth part shows some statistical context of earthquake density development and sketches an approach to analyse individual faults.

3 MRP status 10th of December 2017

MRP status					
	10 December 2017	1 Dec 2017/ vorige periode	Grenswaarden		
			Waakzaamheid	Signalering	Interventie
Activity Rate (# earthquakes, M ≥ 1.5)	17	15	15	20	25
EQ density (# x km^{-2} jr^{-1}, M ≥ 1)	0.27	0.24	0.17	0.25	0.40
PGA (in "g")	0.009 (Zandt)	0.04 (Slochteren)	0.05	0.08	0.10
PGV (most recent maximum, in mm/s)	0.9 (Zandt)	6.4 (Slochteren)	5	50	80
Damage State	DS1	DS1	Δ (model, actual)		
Other patterns	Loppersum M≥1 trend	Loppersum M≥1 trend	"Expert judgement"		

Table 1 MRP status on December 10th 2017.

The activity rate fluctuates around the alertness level (waakzaamheidsniveau). Earthquake density has crossed the signalling level (signaleringsniveau) and has been fluctuating around that level for the last couple of months. The maximum PGA associated with the recent 't Zandt earthquakes was relatively low and stayed far below the alertness level. The measured PGA was also lower than the most recent $M_L \geq 2$ earthquake (Slochteren). The maximum PGV associated with the 't Zandt earthquake was also low and remained below the alertness level. There are no indications for an anomalous development in building damage. No unusual patterns have been observed in the location of earthquakes, the ratio between small and bigger earthquakes or in the relation between earthquake magnitude and PGV/PGA.

4 Earthquake density

The earthquakes that contributed to an exceedance of earthquake density are shown in table 2 and figure 1.

Location	Date	Magnitude
't Zandt	10 Dec 2017	2.1
't Zandt	6 Dec 2017	1.8
Zeerijp	1 Dec 2017	1.3
Zeerijp	1 Dec 2017	1.7
Kantens	15 Oct 2017	1.0
Zandeweer	1 Sept 2017	1.1
Garsthuizen	14 Aug 2017	1.2
Loppersum	25 Jul 2017	1.0
Kantens	21 Jul 2017	1.1
Zeerijp	11 Mar 2017	2.1
Wirdum	26 Feb 2017	1.4
Zandeweer	26 Feb 2017	1.2
Loppersum	25 Feb 2017	1.3
Zijldijk	19 Feb 2017	1.4
Startenhuizen	15 Feb 2017	1.6
Startenhuizen	12 Feb 2017	1.3

Table 2 Earthquakes in the Loppersum area that contributed to the exceedance of the earthquake density threshold value.

This set of earthquakes is largely the same set that contributed to the exceedance of the earthquake density earlier this year. And that is in turn the result of the Quartic Kernel methodology chosen, using a fairly large search-radius and time horizon including earthquakes from within a circle with a radius of 5 km for a period of about a year (see also section 10 for more discussion, or reference 1).

This choice of calculation method for earthquake density leads to a deliberate early and potentially often triggering of this MRP parameter with the intent of early picking up signals of changing subsurface conditions (the other intent of this parameter is to simply pick up an increase of concentration of earthquakes in a certain area without special underlying cause but potentially causing nuisance nevertheless). This means, however, that an exceedance of this earthquake density threshold always needs to be judged in the context of other seismicity developments; in this case it is suggested that the current exceedance is related to the general increase in seismicity in the Loppersum area as already highlighted in reference 2.

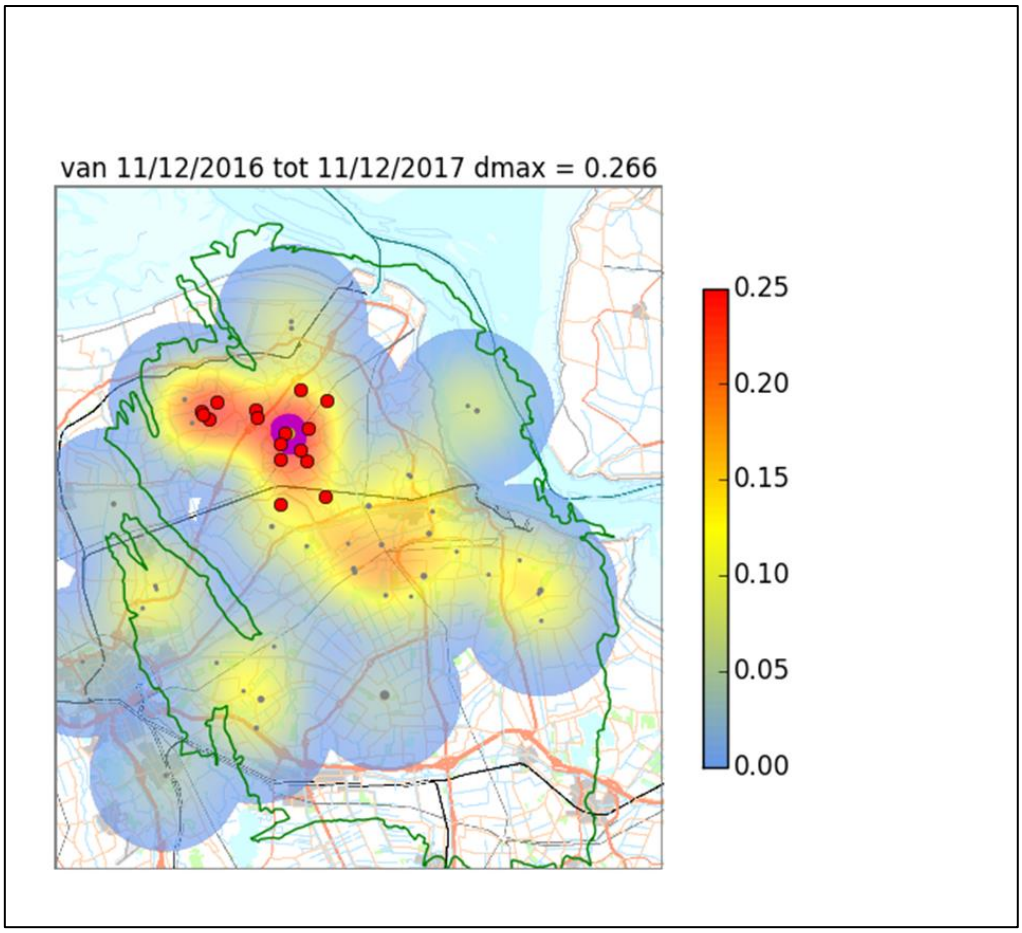

Figure 1 Earthquake density values for the Groningen Field. Colours indicate Earthquake density values. The red dots indicate the earthquakes that contribute to the exceedance of the signalling level.

Figure 2 shows the temporal development of earthquake density in the area. The upper panel with the three maps shows the evolution of the earthquake density for recent times over the Groningen field. The lower left panel shows maximum values for specific locations over a much longer period and it shows that although the values for earthquake density have been increasing over the last year, values have been much higher around 2007 and 2014 for (e.g.) the Wirdum area.

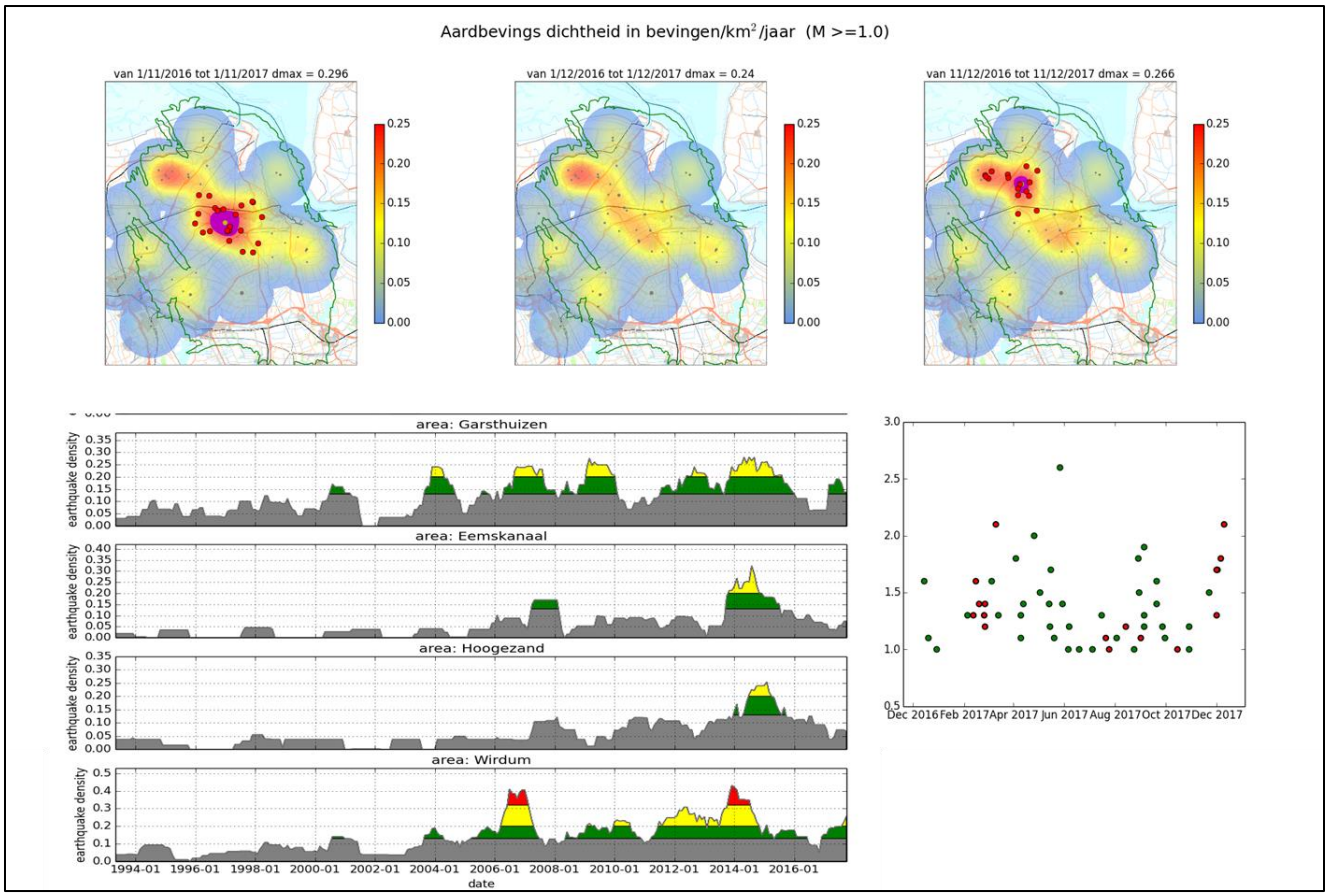

Figure 2 *Evolution of the earthquake density map over time. Red dots in lower and upper panels indicate earthquakes that contribute to the exceedance of the threshold value.*

5 Event rate

The same two earthquakes at 't Zandt also caused the activity rate to increase again above the alertness level, as shown in figure 3. The upper panel shows the observed 12-months number (blue line with blue circles), the alertness level (15, green dashed line) and the expected number from modelling (lighter blue). The lower panel shows the evolution of this activity rate (12 months number) over a much longer period (from 2000 onwards) and shows that the current number is higher compared to 2016 but fairly low compared to 2006 and 2012-2015.

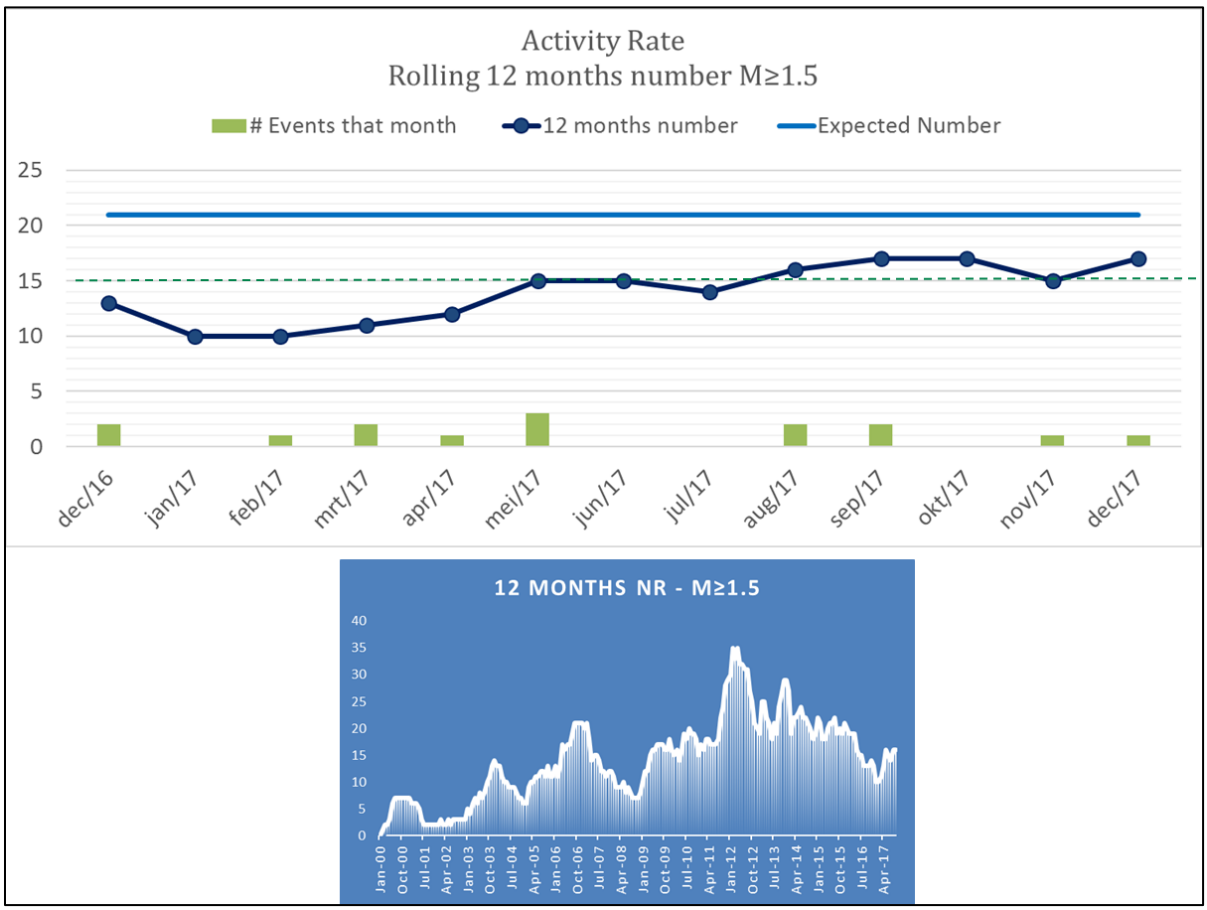

Figure 3 Temporal evolution of the activity rate for the last 12 months. The activity rate has increased somewhat in the first part of 2017 and fluctuates around the alertness level (15). Lower panel shows development of activity rate over a much longer time period (from 2000 to 2017).

6 PGA and PGV

6.1 PGA and PGV in MRP context

Figure 4 shows the PGA value associated with the 't Zandt (2.1) earthquake. It shows that this earthquake caused a relatively low PGA (0.009 g), remaining far below the alertness level (green line).

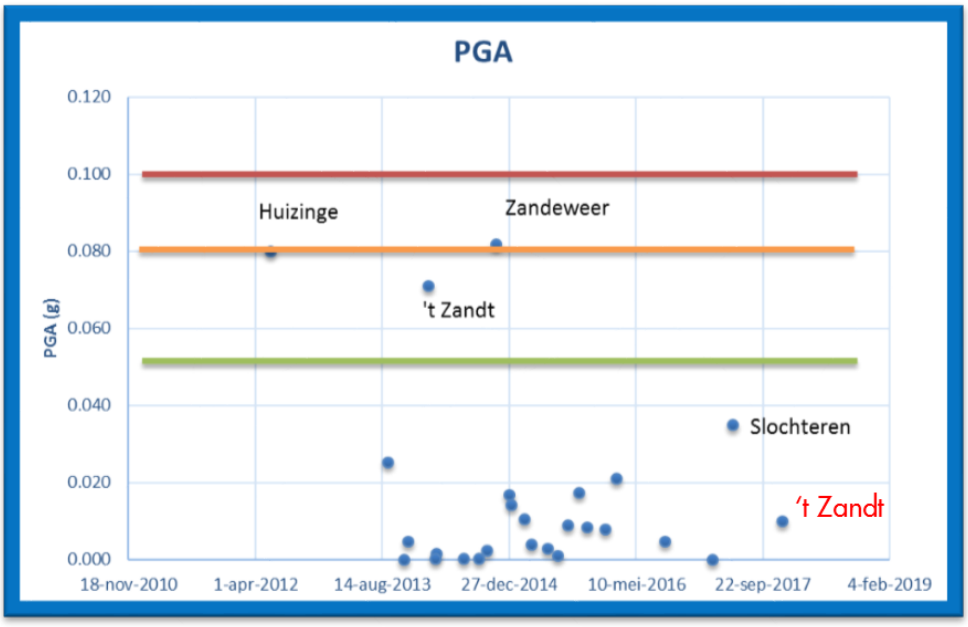

Figure 4 Historical plot of PGA values observed in the Groningen field (M≥2.0). The most recent 't Zandt earthquake (M 2.1, 10th of December) showed a fairly low PGA value.

Figure 5 shows the PGV value for the most recent 't Zandt earthquake. The PGV value of 0.09 mm/s was a relatively low one (is also unlikely to have caused any damage, but that is not the topic of this report).

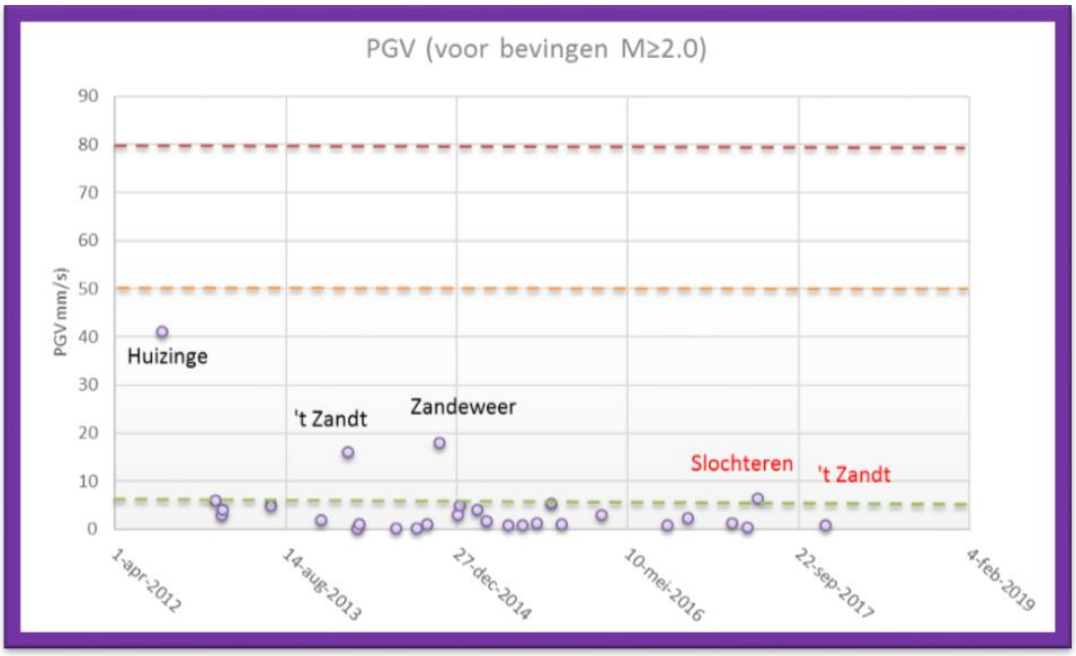

Figure 5 Historical plot of PGV values observed in the Groningen field (M≥2.0). The most recent 't Zandt eartquake (M 2.1, 10th of December) showed a fairly low PGV value

6.2 PGA and PGV analysis

Figure 6 shows the epicentral locations of the two earthquakes (green stars), together with the epicentres of earthquakes of $M_L \geq 2.5$ included in the V5 GMM database (red stars; reference 3) and those of smaller events added for the derivation of an empirical PGV model (blue stars; reference 4).

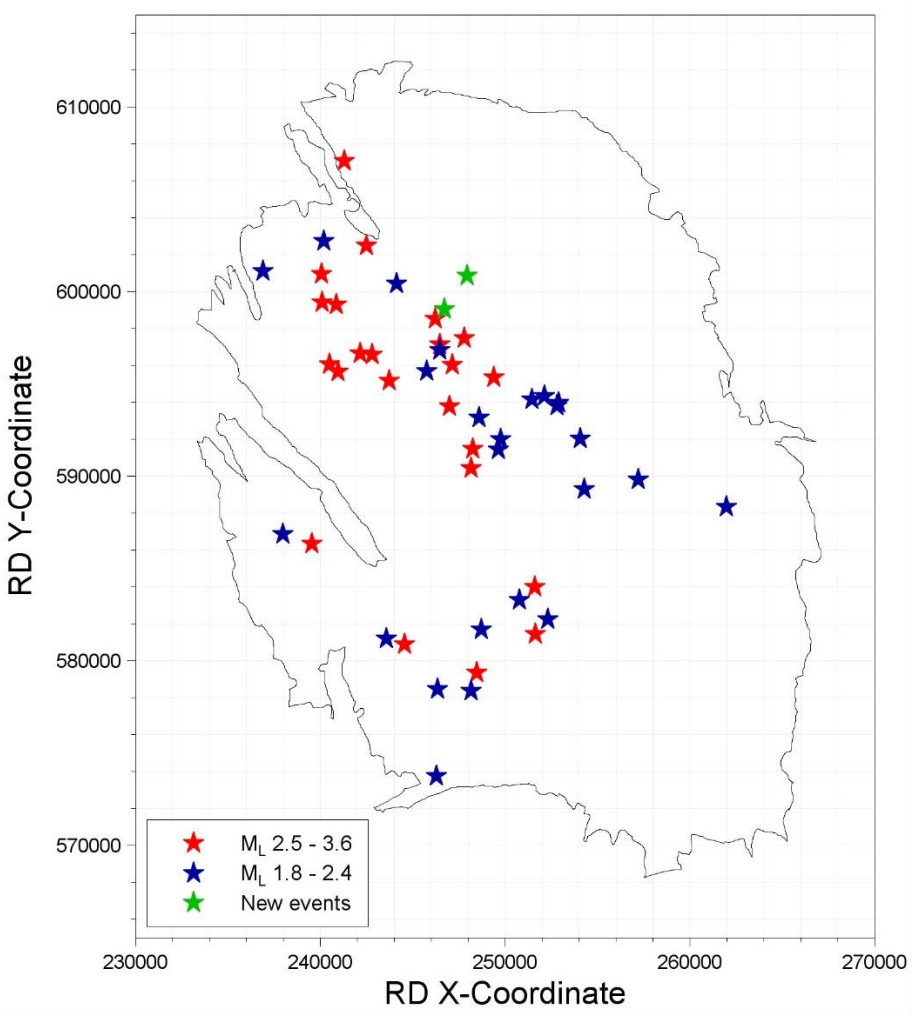

Figure 6 Epicentres of the December 2017 earthquakes (green stars) together with those of earlier events in the Groningen ground motion database

Recordings of the two events have been downloaded from the KNMI portal. After inspecting the records individually, to check for any instrument malfunction and then processing the records through the application of suitable band-pass filters, a total of 73 useable records were retrieved for the first event and 74 for the second event. These include records from the permanent KNMI surface accelerograph network (B-stations) and the surface accelerographs co-located with the borehole geophone network (G-stations). The number of recordings of each event, combined that these included some very close to the earthquake source, means that in both cases the ground motion field has been well sampled by the recording networks.

Details of the maximum horizontal amplitudes of the recorded motions are summarised in Table 3. As can be appreciated, the largest recorded values of PGA on a single component were equal to 0.004*g* and 0.009*g* respectively in the two earthquakes, both recorded at the same station. The corresponding values of PGV were 0.073 cm/s and 0.095 cm/s. As would be expected for such small magnitude earthquakes, these amplitudes are very low and well below thresholds considered to be potentially damaging. The largest amplitude recorded during the larger (M_L 2.1) earthquake at a distance of just over 1 km from the epicentre was less than 1% of the acceleration due to gravity.

M_L	No Rec.	Maximum PGA_{GM} (cm/s^2)	Maximum PGA_{Larger} (cm/s^2)	Maximum PGV_{GM} (cm/s)	Maximum PGV_{Larger} (cm/s)	Maximum PGV_{MaxRot} (cm/s)	Station	R_{epi} (km)
1.8	73	2.52	3.82	0.047	0.073	0.079	G140	3.17
2.1	74	8.29	9.09	0.089	0.095	0.126	G140	1.33

Table 3 Characteristics of largest amplitude recordings (GM: geometric mean of horizontal components; Larger: larger as-recorded horizontal component; MaxRot: largest vector component)

Figure 7 shows the geometric PGA values recorded during the two events plotted against distance from the earthquake epicentres. Most observations that can be made with regards to this figure are features that are to be expected, including the fact that the amplitudes from the larger of the two earthquakes are marginally higher. Figure 8 shows the same geometric PGA values from the two earthquakes plotted against magnitude together with the PGA values obtained from the 45 earthquakes used to derive the empirical PGV model for the field (reference 4). This figure suggests that in general the amplitudes of motion from these two events are generally consistent with those observed in earlier events; the single isolated maximum values visible for both events probably reflect, more than anything else, the benefits of the expanded recording networks capturing more readily the very near-source amplitudes of shaking. Even these peaks, however, are unexceptional within the context of the general levels of recorded motions. Figure 9 shows the individual horizontal components of PGA plotted in the same way but now grouped by distance ranges. These plots confirm that the recorded values from the recent events are consistent with those from earlier events; if anything, the general position of the amplitudes from the more distant recordings (> 10 km) would even suggest that the events are slightly weaker than average.

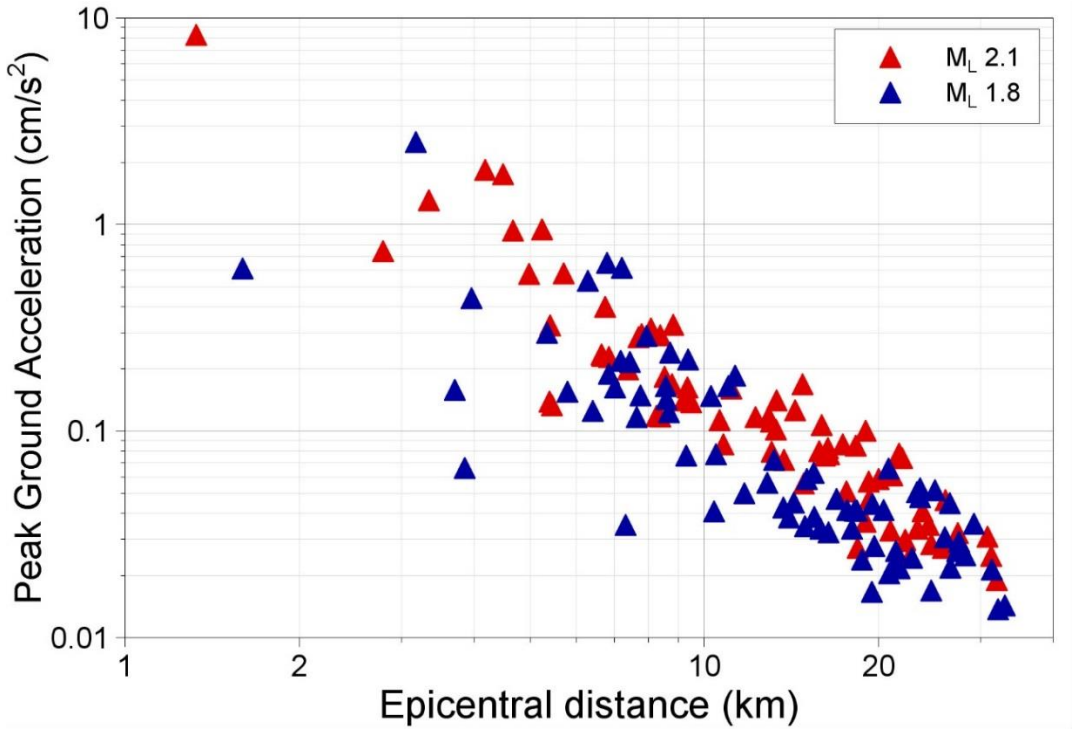

Figure 7 Geometric mean horizontal PGA values from the two 't Zandt earthquakes plotted against epicentral distance

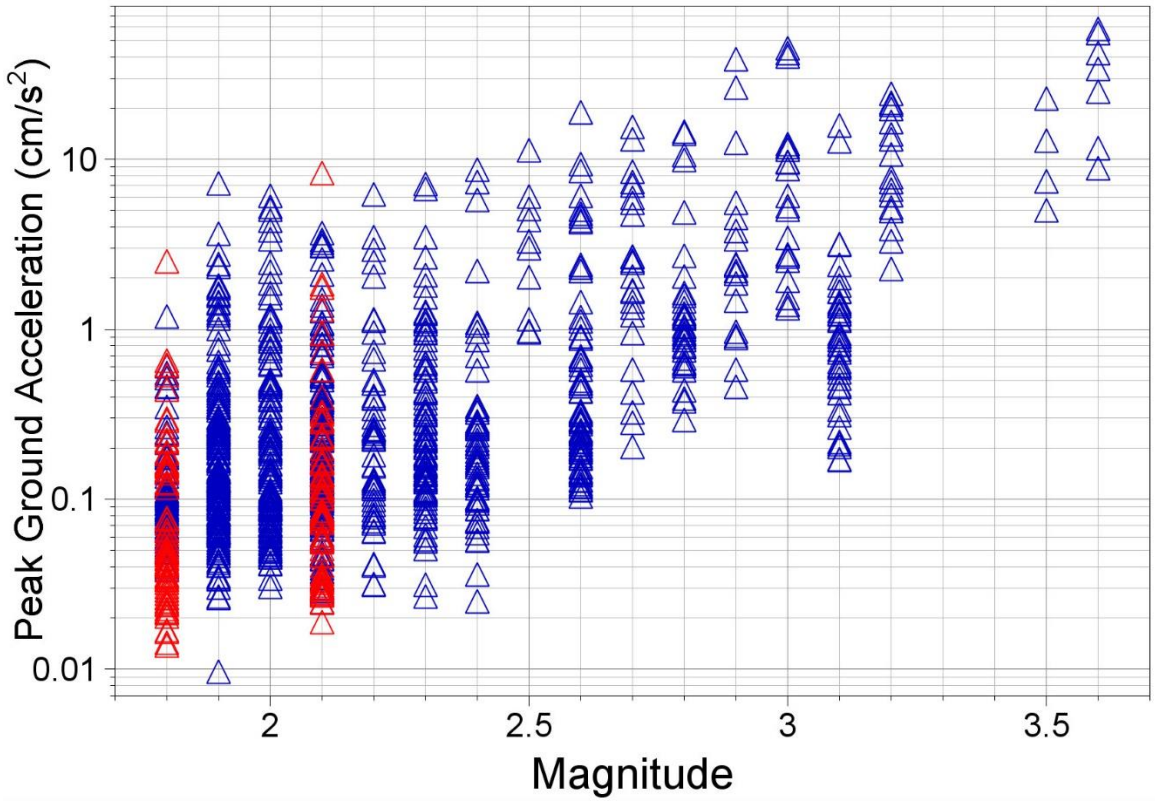

Figure 8 *Geometric mean horizontal PGA values from the two 't Zandt earthquakes plotted against magnitude together with the PGA values from the 45 earthquakes in the database used for the empirical PGV model; note that at several magnitudes, particularly in the lower range, there are data points from multiple earthquakes*

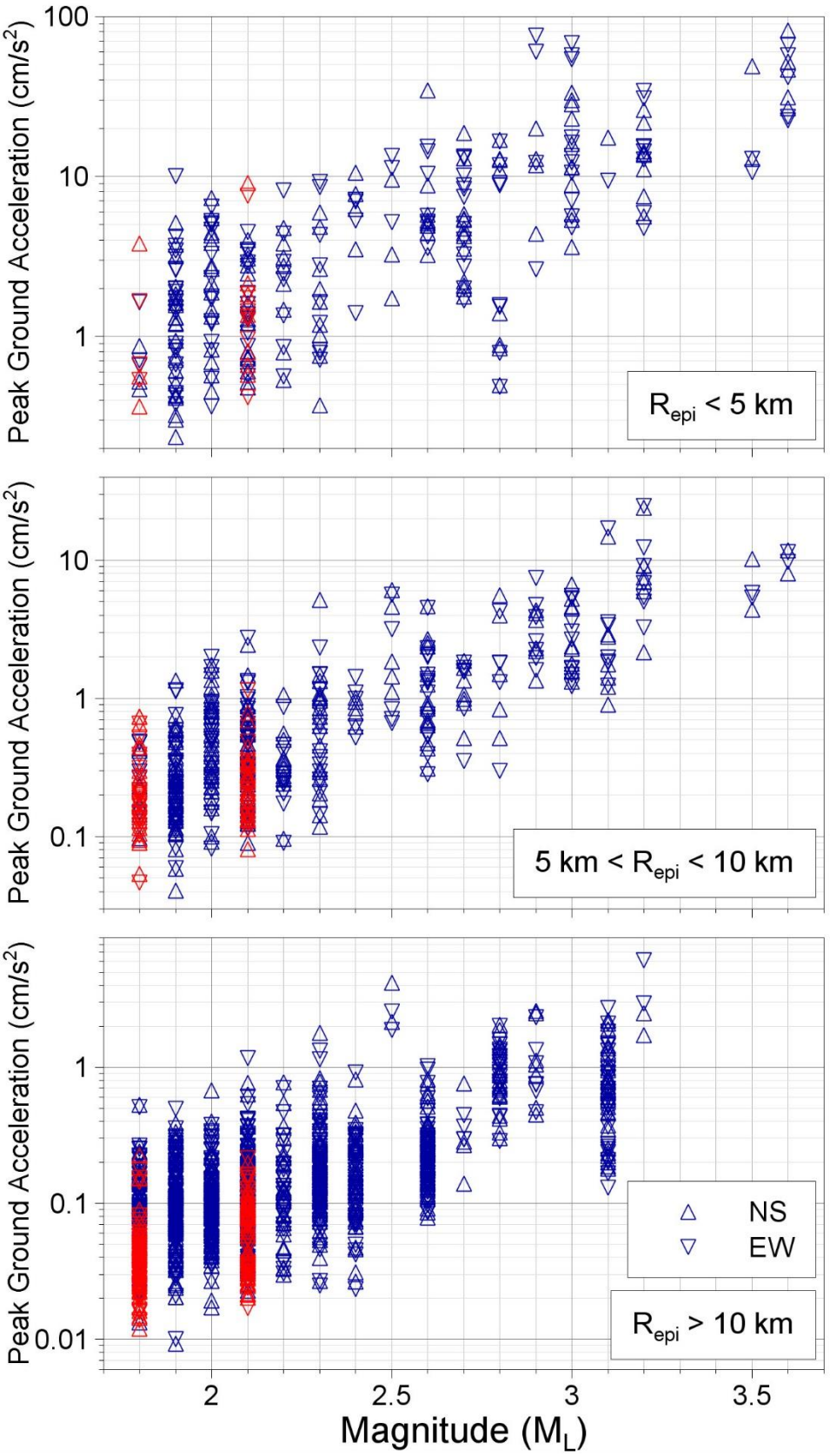

Figure 9 *Individual horizontal PGA components from the two 't Zandt earthquakes plotted against magnitude together with the PGA values from the 45 earthquakes in the database used for the empirical PGV model, grouped by ranges of epicentral distance; note the different y-axis scales on the three plots*

In terms of PGV values, Figure 10 shows the recorded peaks from the two events against distance. Here we plot three different definitions of the horizontal PGV: (bottom) the geometric mean of the two orthogonal recordings (consistent with the Groningen ground motion model), (middle) the larger of the two, and (top) the maximum rotated component. The latter two are included to cover the V_{TOP} definition, the definition of which is somewhat ambiguous but which likely corresponds to one of these options. An interesting observation that can be made from Figure 11 is that the shape of geometric spreading adopted for the ground motion model—and confirmed by full waveform simulations—is clearly visible: there is an initial steep decay out to distances of about 7-8 km, followed by an interval of no decay (or even a possible increase in amplitudes, which would be due to simultaneous arrivals of direct and refracted waves) out to about 12 km, after which there is a more gradual decay. Another interesting observation that can be made is that the only PGV to exceed 1 mm/s is obtained by rotating the horizontal components of the closest recording to the source to obtain the orientation at which the velocity peak is maximal.

Figure 11 shows the geometric mean PGV values from these two recent earthquakes plotted against magnitude with the PGV values from the current ground motion database. As for the PGA values plotted in Figures 8 and 9, it can be seen here that there is nothing unusual about the amplitudes of the motions from these events when compared to those from previous earthquakes in the field. Again, if anything, the amplitudes on average may appear to be somewhat lower than average.

To explore where the amplitudes of these motions actually lie with respect to average levels of motion in the field to date, the residuals of PGV have been calculated with respect to the empirical prediction equations recently derived using all of the blue data points in Figure 12 (reference 4). The results are shown in Figure 13 for all three horizontal component definitions. The plots show the between-earthquake (inter-event) residuals against magnitude and the within-earthquake (intra-event) residuals against epicentral distance. The patterns are consistent with other Groningen events in terms of the spatial variability—which seems to be greatest at short distances although this may also be related to data density—but it can be seen that for both earthquakes there are strong negative event terms, confirming that the amplitudes are lower than average when compared to the motions from the 45 earlier earthquakes in the current ground motion database. This is consistent with the trend that has been noted that the most recent earthquakes are all showing negative event terms (Figure 13), which would generally be interpreted to imply that the stress drops from these more recent events are lower than those of earlier events. No explanation has yet been postulated for why there may be this apparent trend for weaker seismic sources in recent times.

To complete the report, Figure 14 shows the horizontal component traces and Husid plots for the strongest recording in both earthquakes (from station G140) from which it can appreciated that, as always, the high amplitudes are associated with very short durations of motion.

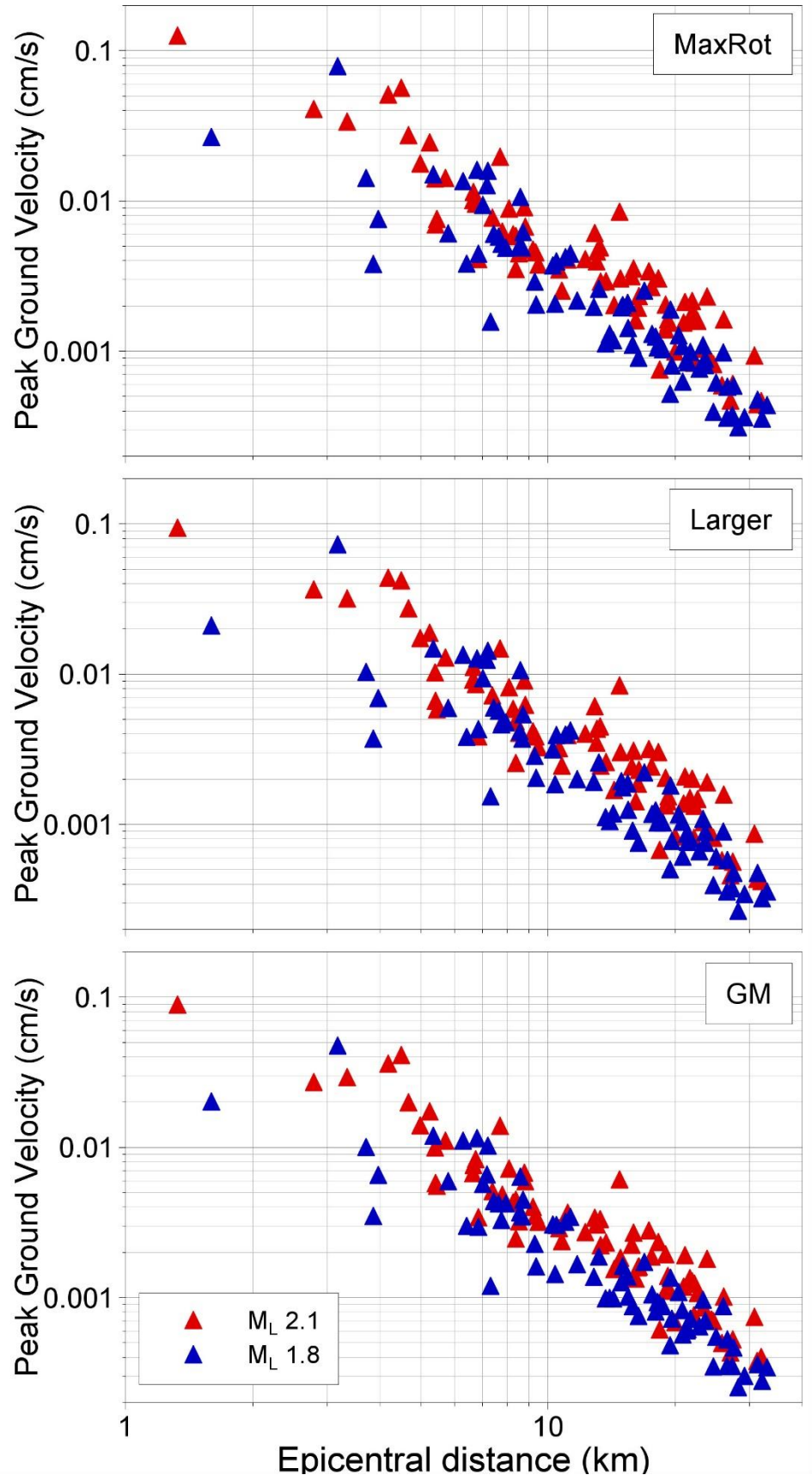

Figure 10 Horizontal PGV values from the two 't Zandt earthquakes plotted against epicentral distance using three different component definitions: Top: maximum rotated; middle: larger recorded; bottom: geometric mean.

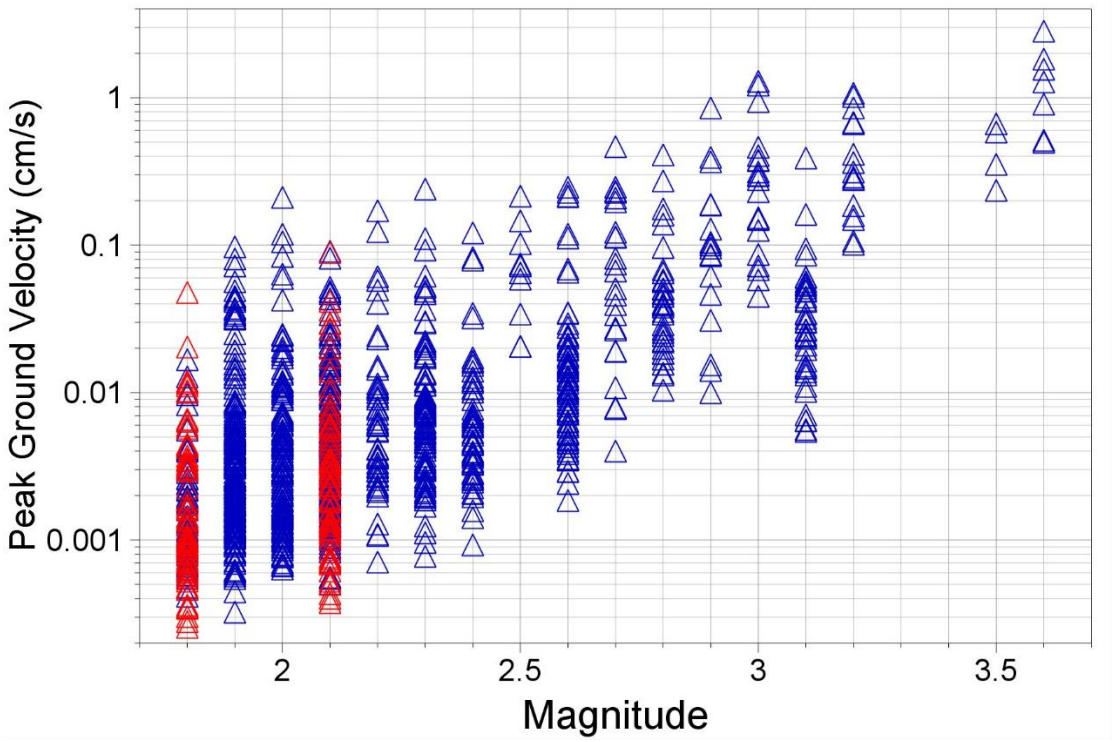

Figure 11 Geometric mean horizontal PGV values from the two 't Zandt earthquakes plotted against magnitude together with the PGV values from the 45 earthquakes in the Groningen database

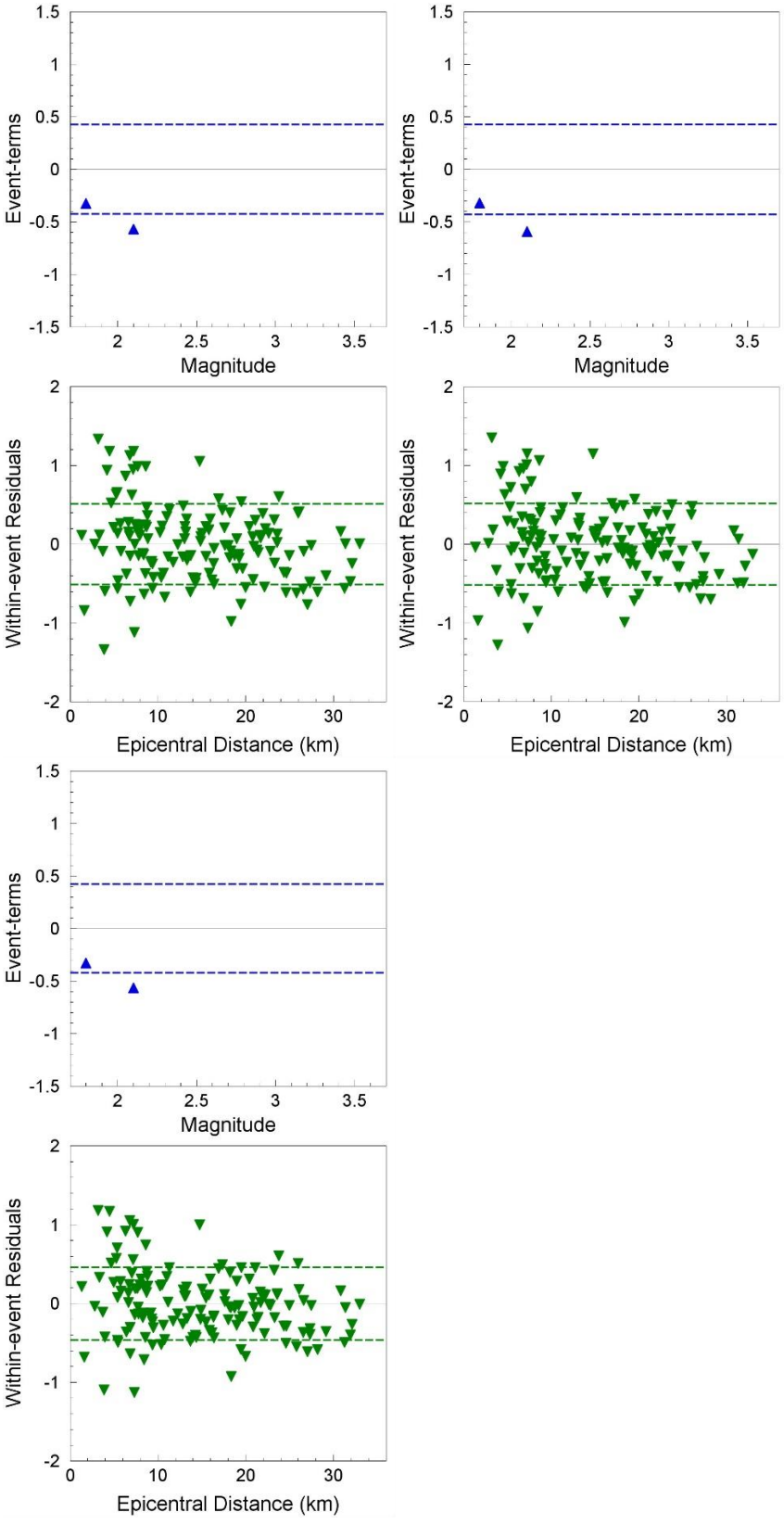

Figure 12 Residuals of recorded PGV values from the two recent events calculated with respect to the empirical PGV equations for the Groningen field. Left: maximum rotated; middle: larger recorded; right: geometric mean.

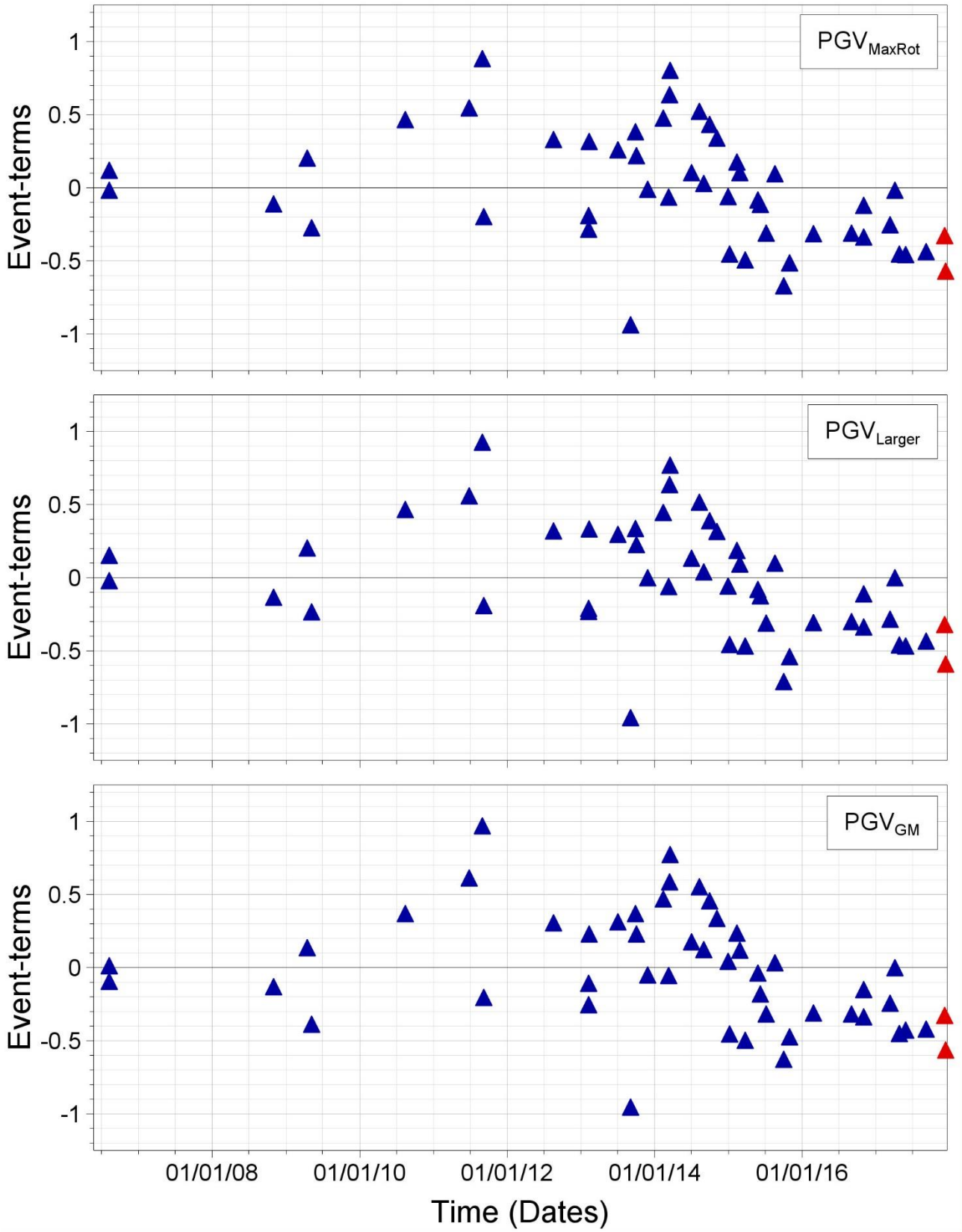

Figure 13 Event terms for geometric PGV predictions calculated with respect to the empirical PGV models for Groningen, plotted against date of the earthquake, with the recent 't Zandt events shown in red. Top: maximum rotated; middle: larger recorded; bottom: geometric mean.

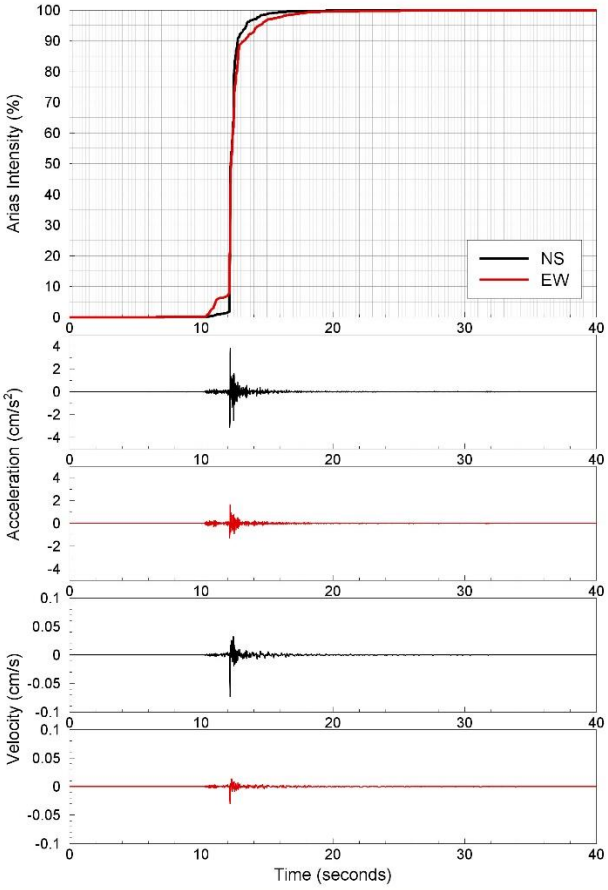
Arias Intensity (%)
NS
EW
Acceleration (cm/s²)
Velocity (cm/s)
Time (seconds)

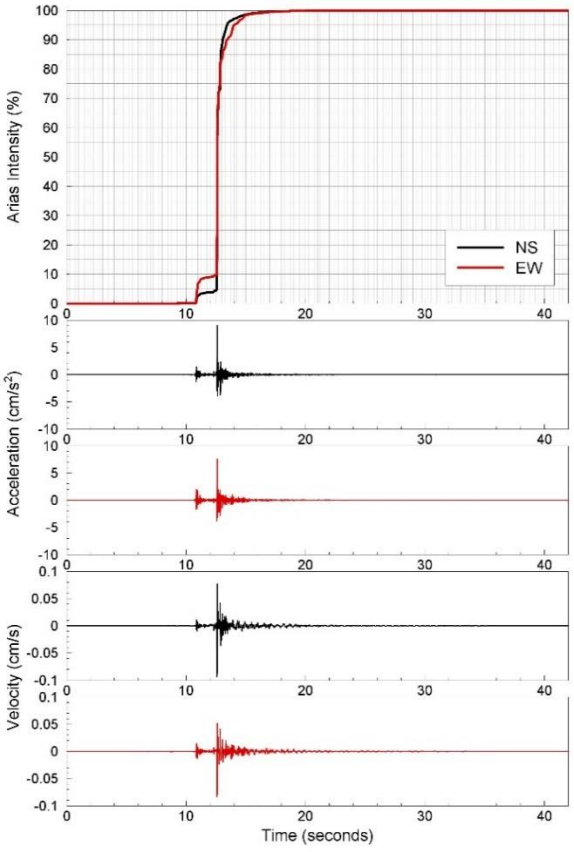
Arias Intensity (%)
NS
EW
Acceleration (cm/s²)
Velocity (cm/s)
Time (seconds)

Figure 14 Horizontal traces of acceleration and velocity recorded at the G140 accelerograph station, together with Husid plots showing the build-up of Arias intensity over time. Left: M_L 1.8 event of 6 December; right: M_L 2.1 event of 10 December.

In summary, these two recent earthquakes have been exceptionally well recorded and the amplitudes of motion are consistent with those from previous earthquakes of comparable magnitude but somewhat lower than average. The very low amplitudes of the shaking combined with the extremely short durations make these ground motions of little significance to the built environment. Indeed, these small magnitude earthquakes are primarily significant from the perspective of disturbance to the local population.

7 Further analysis ‘t Zandt earthquakes

In this section, some analysis will be presented on the last two earthquakes at ‘t Zandt with two objectives in mind:

1. Assessing whether an unexpected development in seismicity has been observed.
2. Assessing whether useful data can be obtained for ongoing research on seismicity development on individual faults or fault junctions

7.1 Overview of earthquakes in the ‘t Zandt area

Figure 15 shows the history of earthquakes in the ‘t Zandt area for earthquakes with a magnitude of 1.5 and higher. The table in the upper corner shows a list of these earthquakes. The black lines show the subsurface position of faults projected on the surface (topographic map). The highest magnitude earthquake in this area seems to have been associated with the larger NW-SE running fault whereas the most recent earthquake hypocentres plot on relatively minor existing faults (see also sections below).

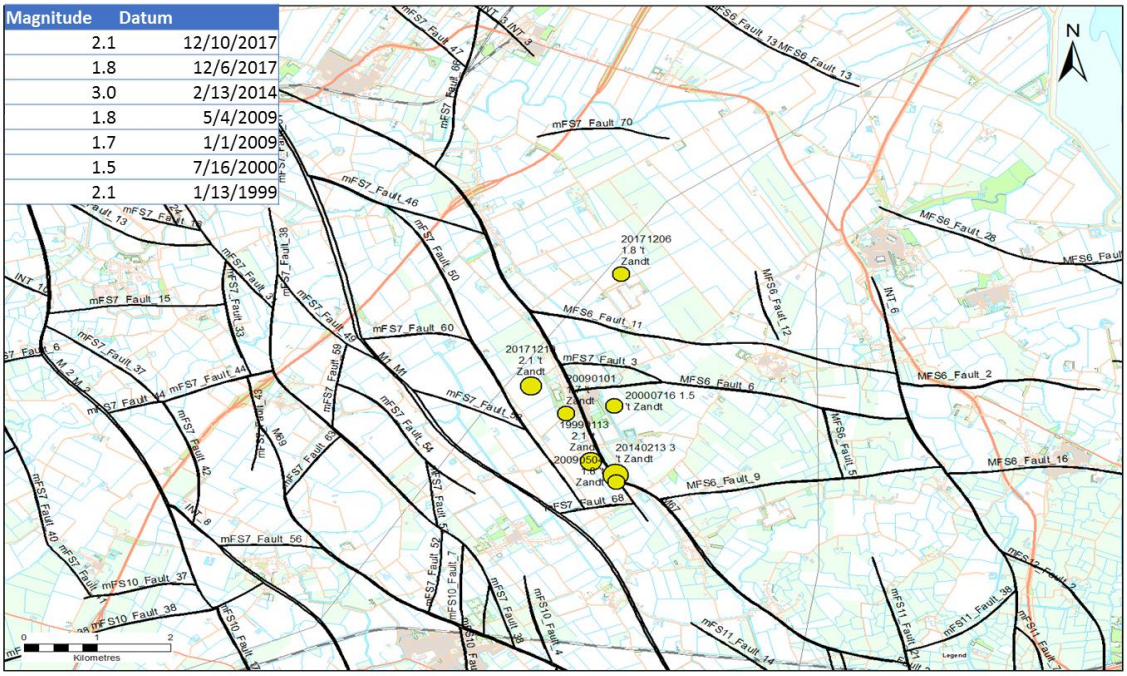

Figure 15 Epicentres of all ‘t Zandt earthquakes with a magnitude of M≥1.5. Black-lines are the faults at about 3 km depth (these faults terminate in the Zechstein Formation and do not continue to surface).

7.2 Hypocentre location

Figure 16 shows the hypocentre location of the two ’t Zandt earthquakes as derived from the Full Waveform Inversion workflow (reference 3). In this Full Waveform Inversion workflow not only the first arrival time picks of P-waves are used, but the full recorded seismic signal, including the S-wave waveforms is used. With the aid of a detailed 3D local velocity model (derived from available 3D seismic data and sonic logs), a quite accurate hypocentre location can be determined, including depth. As can be seen on the map plots, the epicentres determined by this method have been shifted some 900 m to the south, relative to the original KNMI location. Now the epicentres are coinciding with certain mapped faults in the field.

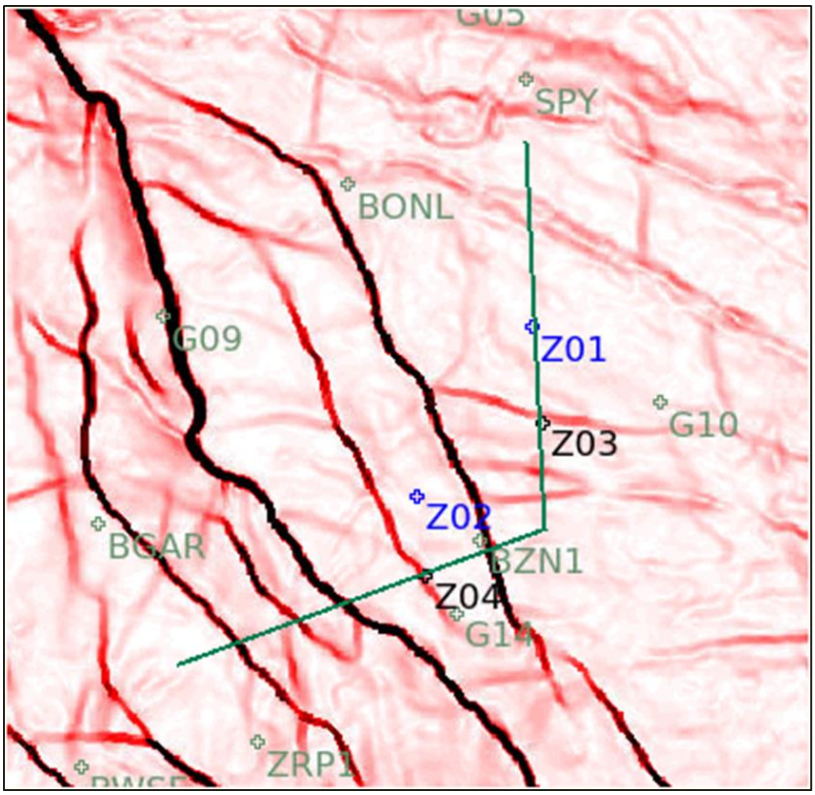

KNMI epicentres:
Z01: 06-12-17, M=1.8
Z02: 10-12-17, M=2.1

Shell epicenters
Z03: 06-12-17, M=1.8
Z04: 10-12-17, M=2.1

Figure 16 Hypocentre location of the two 't Zandt earthquakes.

Figure 17 shows a cross-section along the green line in figure 16. The earthquakes are shown to plot on "fault 1" and "fault 3".

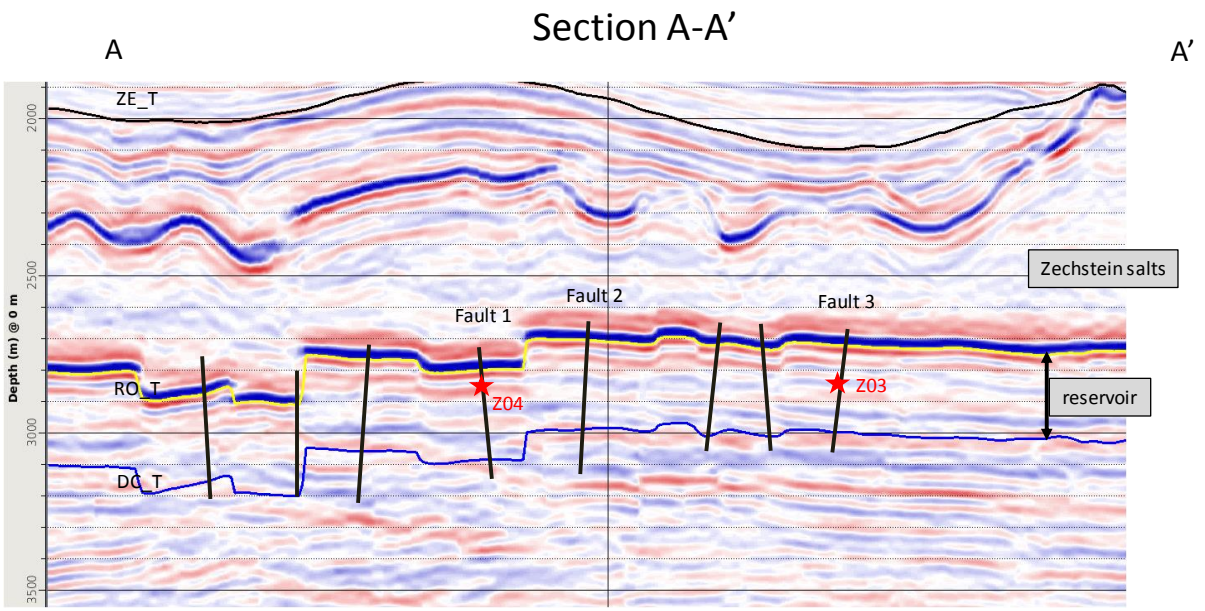

Shell epicentres: Z03: 06-12-17, M=1.8, depth 2850 m.
Z04: 10-12-17, M=2.1, depth 2850 m.

Figure 17 Cross-section as indicated by the line in figure 16. Hypocentre location of the two 't Zandt earthquakes

8 Historical context, trends and forecast

Figure 18 shows the number of earthquakes in the Loppersum and East areas for earthquakes with a magnitude of 1.5 and higher (see for area definitions, reference 2). For both areas holds that the current seismicity level is low compared to 2011. The Loppersum area, however, shows a recent increase in seismicity (despite production minimalized, see also reference 2 for discussion). The East area, in contrast has not shown this upward increase.

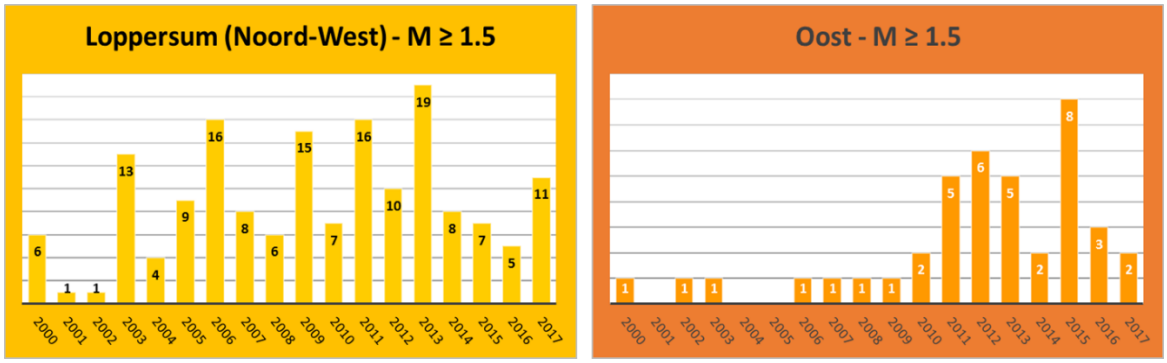

Figure 18 Yearly number of earthquakes for the Loppersum area and for area "East". The Loppersum area shows a recent increase whereas the "East" area still shows a relatively low number of earthquake (see also reference 2).

Figure 19 shows the monthly numbers for the Loppersum area for two magnitudes in the upper two panels. The lower two panels show the forecasted number of earthquakes in the area (see also reference 2). The left lower panel shows a machine learning (Random Forest) forecast indicating a relatively flat, even somewhat declining base-case forecast (see reference 2 for more discussion). The lower right panel shows a forecast from the hybrid geomechanical-statistical model showing a very slight increase of expected number of earthquakes for the area.

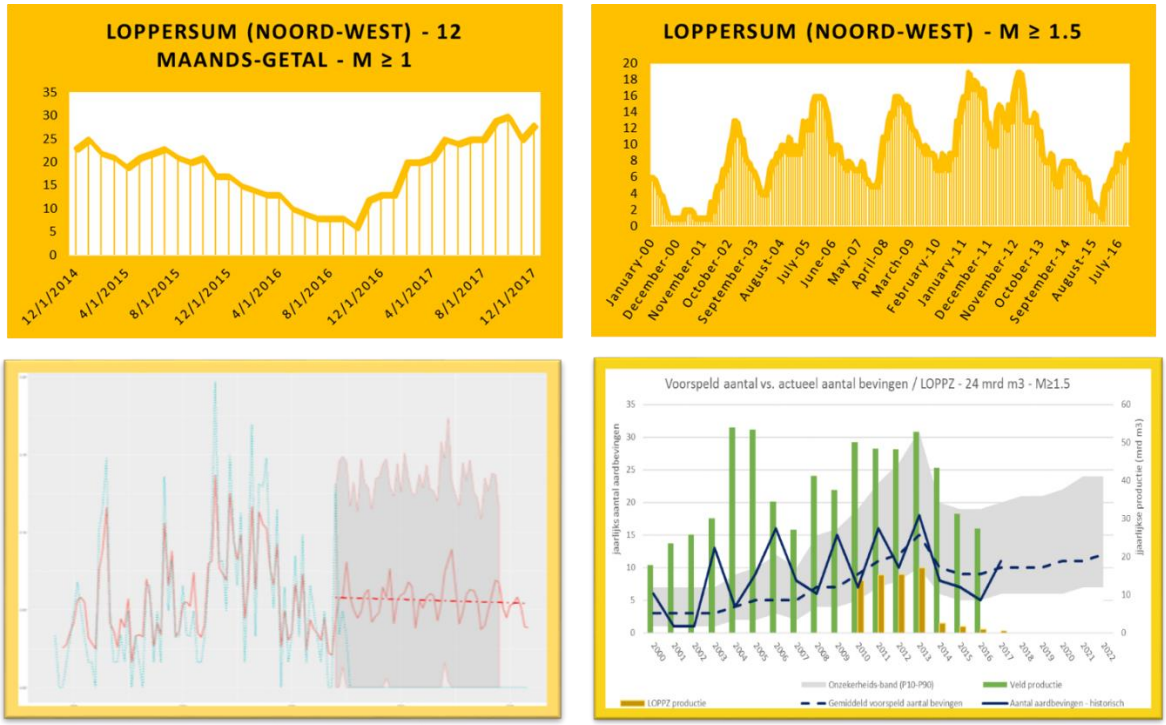

Figure 19 Loppersum observed trends (upper two panels) and forecasts (lower two panels). A full background to this figure is given in reference 2.

9 Production and pressures

In this section, the knowledge of the hypocentre locations of these of these earthquakes will be looked in the context of local production and reservoir pressure development, as reservoir pressure is known to be able to cause stress changes around faults. For the analysis of reservoir pressure, the Groningen Reservoir model (reference 5) is used.

This Groningen reservoir model has been extended with production data through 18th December 2017. The two cluster locations closest to the earthquake epicentres, as shown in section 8, are 't Zandt (ZND) and Leermens (LRM). Daily production during 2017 from these two locations are given in figure 20 a. Given that these clusters fall under the Loppersum cap, the production is very much restricted. Further away from these locations are the clusters Bierum (BIR), Amsweer (AMR) and Overschild (OVS). BIR and AMR are not restricted by the Loppersum cap, with corresponding higher production rates as evident from figure 20b.

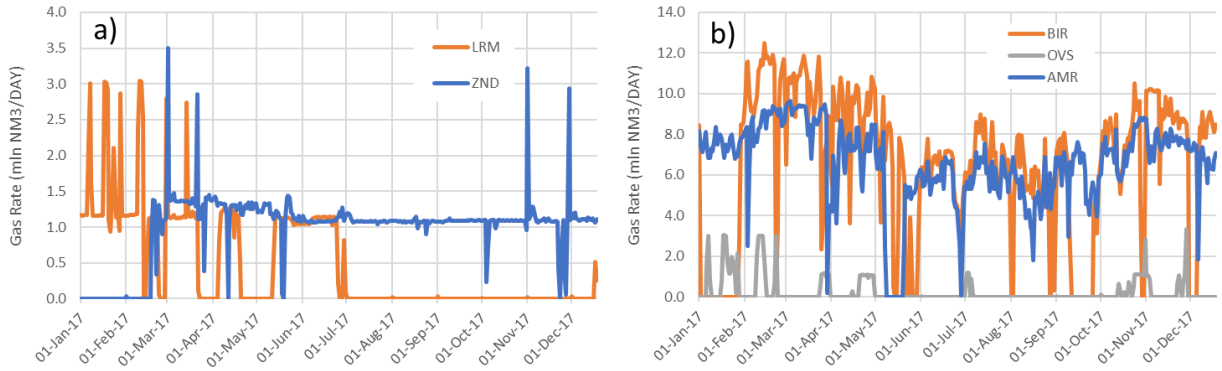

Figure 20 Cluster daily gas production for 2017 for clusters LRM and ZND (a) and BIR, OVS and AMR (b).

The location of the two earthquakes near 't Zandt relative to the reservoir model grid is shown in table 4.

Location	Date	Magnitude	X	Y	Grid Block I	Grid Block J
't Zandt	06/12/2017	1.8	248050	599850	78	95
't Zandt	10/12/2017	2.1	246800	598200	74	91

Table 4 Earthquake location in the MoRes Grid

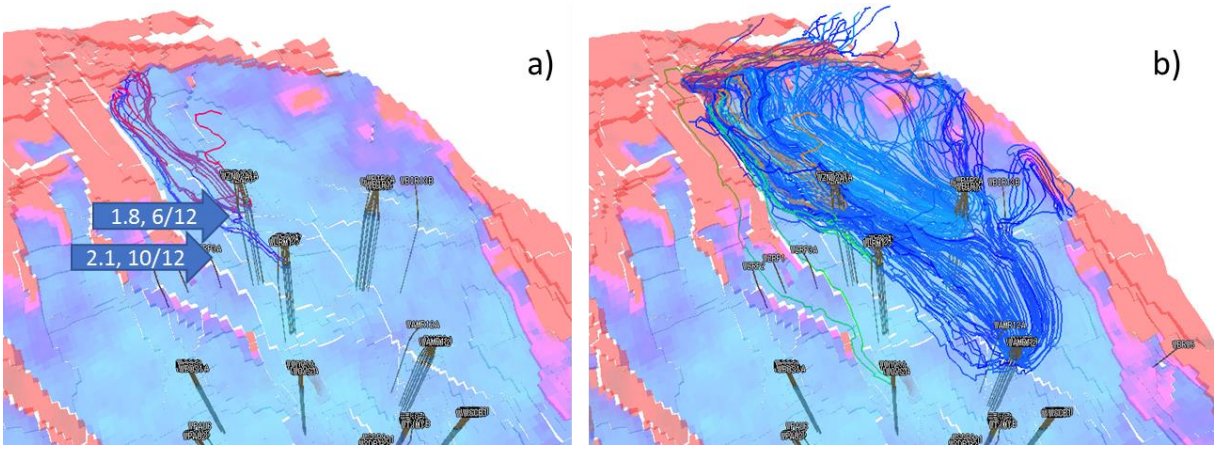

Figure 21 Streamlines, as per mid December 2017, arriving at clusters ZND and LRM (a) and BIR, OVS and AMR (b). Underlying property shown is gas saturation in Upper Slochteren.

In Figure 21 a, the streamlines arriving at these northern production clusters are shown. Given the low production from ZND and LRM, the area drained by these clusters is very small (Figure 21 a) with the AMR and BIR clusters draining the largest area in the North (Figure 21 b). The modelled pressure behaviour at the two earthquake locations are shown in Figure 22. The pressure values shown are daily pore volume weighted averages across the Slochteren formation at the earthquake locations. With gas being a highly compressible fluid, the impact on pressure from production fluctuations at the ZND and LRM locations are quickly dampened out away from the production locations. This is particularly evident in the response at the location of the 10th December event. The pressure derivative remains largely flat throughout the year. The event on the 6th December is reasonably close to the ZND location and this is also evident in the more varying pressure derivative response. For example, the production increases on the 1st and 29th November (see Figure 20) can be observed back in the derivative response.

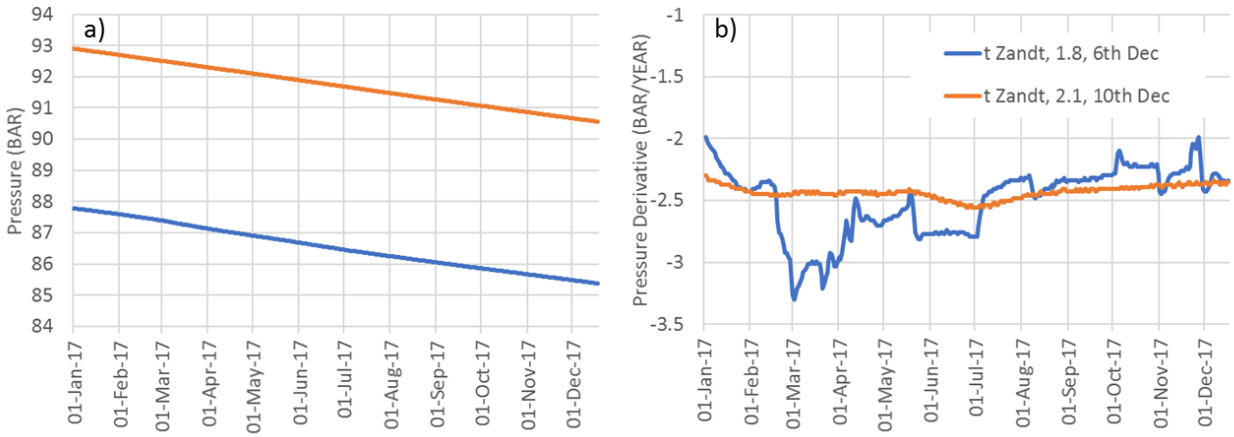

Figure 22 Pressure behaviour at earthquake epicentre locations for the 't Zandt events on the 6th and 10th December 2017.

In figures 23 and 24, the Upper Slochteren pressure in several grid cells are shown. In figure 23 the cells follow a line between the 't Zandt and Leermens locations, crossing the December 6th event. In figure 24 the line is between 't Zandt and Zeerijp, crossing the December 10th event.

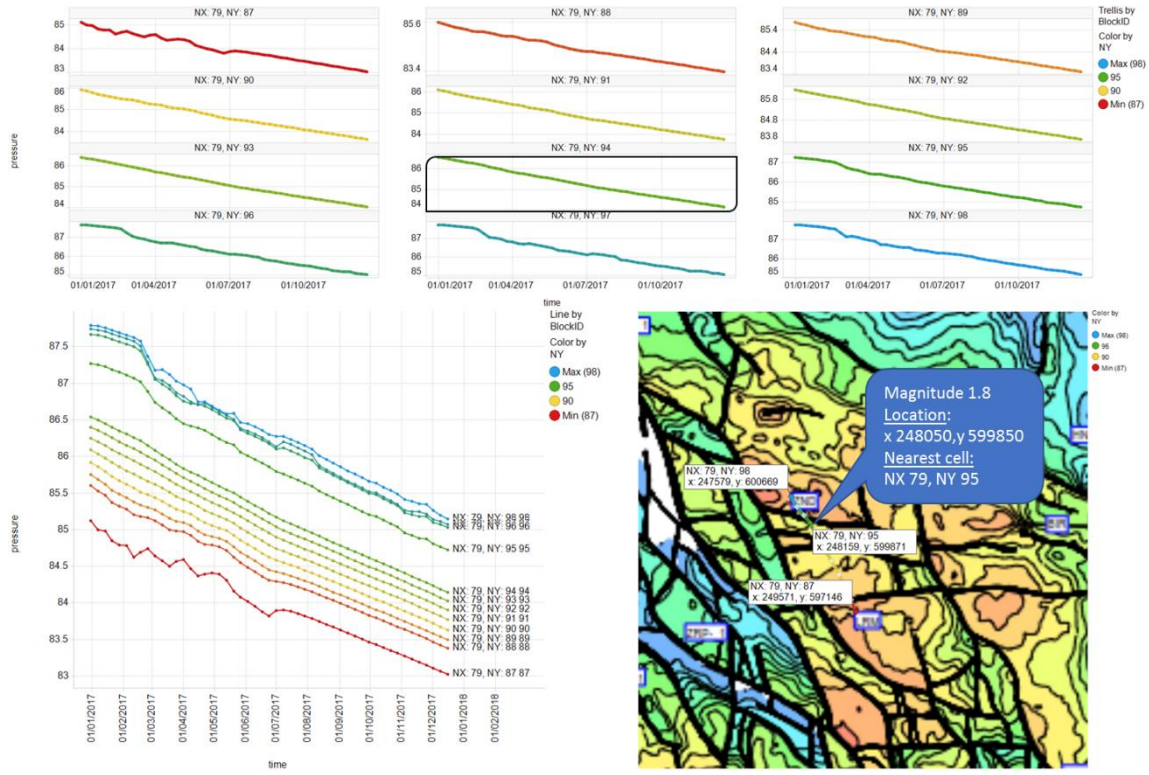

Figure 23 Pressure in the Upper Slochteren for grid cells in a line between 't Zandt and Leermens locations. This line crosses the location of the December 6th event.

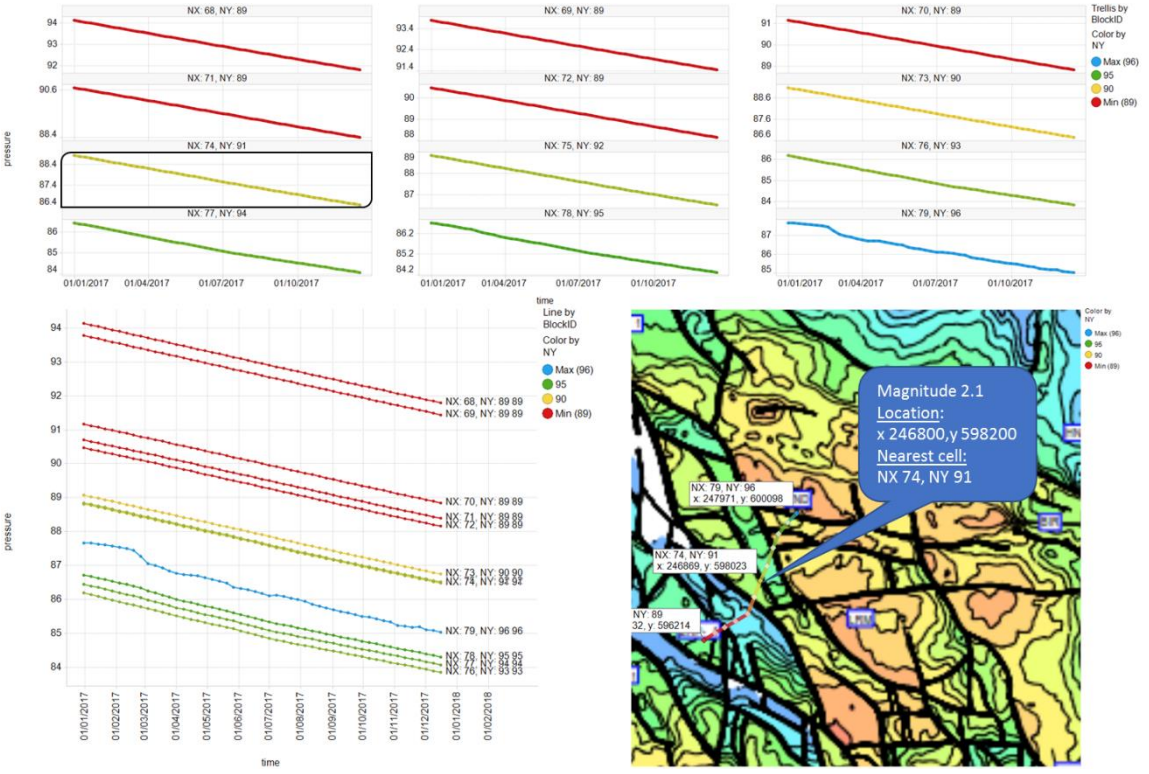

Figure 24 Pressure in the Upper Slochteren for grid cells in a line between 't Zandt and Zeerijp locations. This line crosses the location of the December 10th event.

10 Synthetic time-series of earthquake densities

In section 4 on earthquake density, it was highlighted that it is important to understand whether the underlying driving mechanism for the generation of earthquakes has changed. One way to gain an understanding the theoretical behaviour of this parameter is by simulating its evolution under influence of a statistically varying number of earthquakes in place and time. This understanding will help interpreting observed time-series of earthquake density in future, set expectations for the MRP level we will be in the next couple of years and helps judging the currently observed fluctuations in earthquake density.

10.1 Quartic kernel calculation method for earthquake density

The calculation method for earthquake density in the MRP is adapted from reference 5. The method uses a so-called quartic kernel:

$$\frac{15}{16}\left(1-\left(\frac{x_i}{r}\right)^2\right)^2$$

This quartic kernel with a radius (r) of 5km is applied to all earthquakes with a magnitude of 1 and higher that have taken place during a 12-month period. In this way, the earthquake density can be calculated for every cell (50x50m) for this 12-month period. The current earthquake density period ranges from December 11th 2016 to December 10th 2017. For all 50x50 m cells this calculation is repeated over the entire Groningen field and then the maximum value is reported.

10.2 Generation of hypothetical time-series for earthquake density

A synthetic time-series can be obtained by making the following assumptions:

1. A constant average number of M≥1 earthquakes per month (based on observed number since 2015 = 3.9 per month); note that this does not mean that the actual simulated number per month always equals 3.9 (it almost never does); instead this number varies in this simulation for very month and can assume numbers above and below this average based on probability and is determined by the distribution the sample is drawn from:
2. The number of earthquakes per month is being drawn from a Poisson distribution with a constant average.
3. Synthetic earthquakes obtained in this way are independently from each other assigned a cell based on history:
4. Earthquakes are assigned a location based on the historical geographical distribution of earthquakes (i.e. an earthquake in the Loppersum area is about 9 times more likely to occur than an earthquake between Hoogezand and Winschoten).

10.3 Results synthetic time-series for earthquake density

Based on 1000 draws from the distribution described above the following results are obtained, see figure 25, where 4 synthetic examples of time-series are shown. From this figure, it is clear that fluctuating, declining and even steeply, monotonously increasing patterns can arise from chance only. Even the highest MRP threshold level, the intervention level, can be exceeded from random variations only.

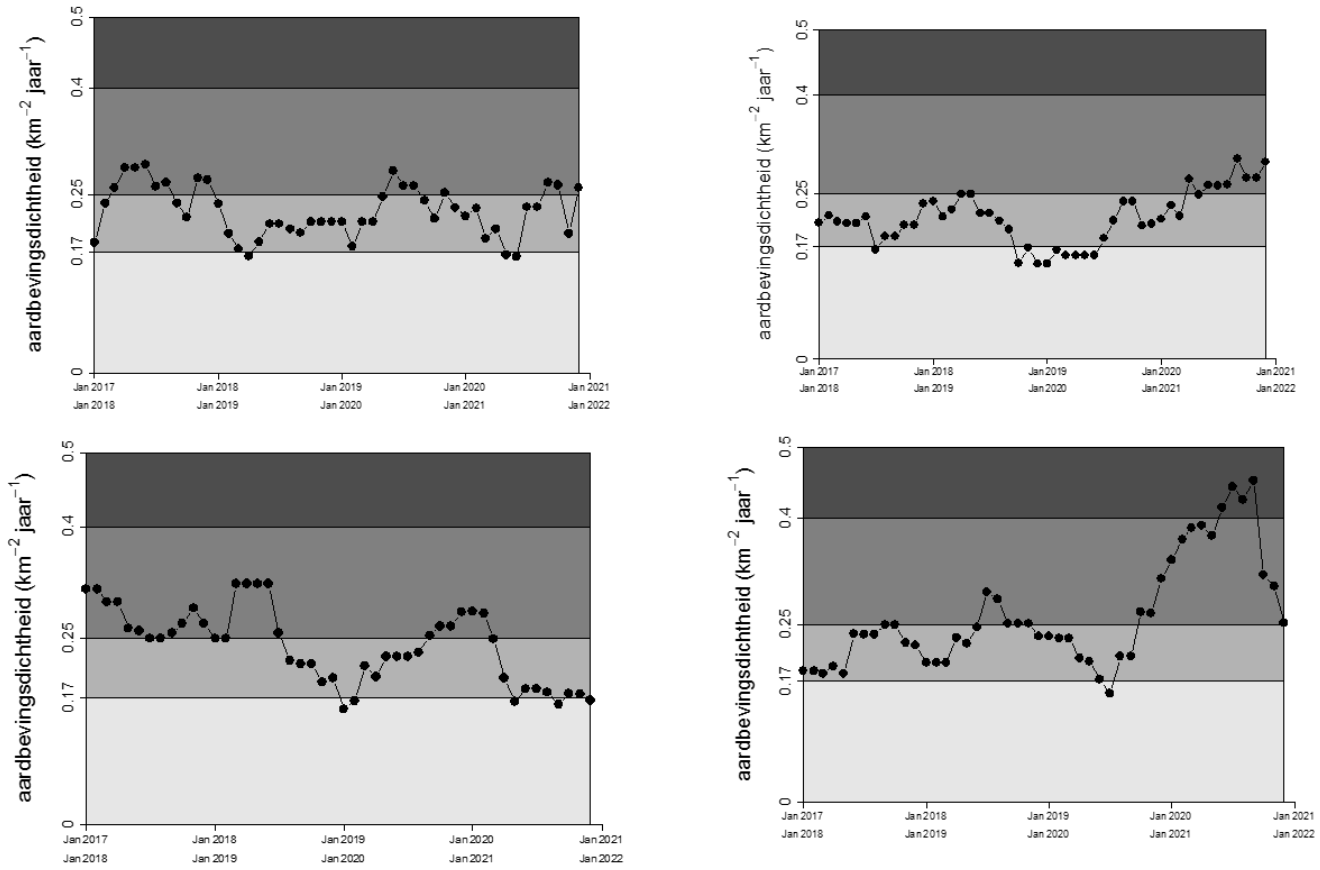

Figure 25 Stochastical simulation of earthquake density. The 4 panels illustrate the probability of exceeding earthquake density without any specific change in subsurface conditions. Maxima per for 4 randomly chosen synthetic catalogues.

Figure 26 shows the yearly probability of exceedance of the three MRP threshold values. The probability of exceeding the intervention level amounts to about 3% per year. The signalling level has a probability of being exceeded of 75% (+3%). So, without any changing conditions in the subsurface, we are most likely to hover between the signalling level and the intervention level. There is (only) a 22% probability that we stay below the signalling level and only a theoretical 0.1% probability that we stay below the alertness level.

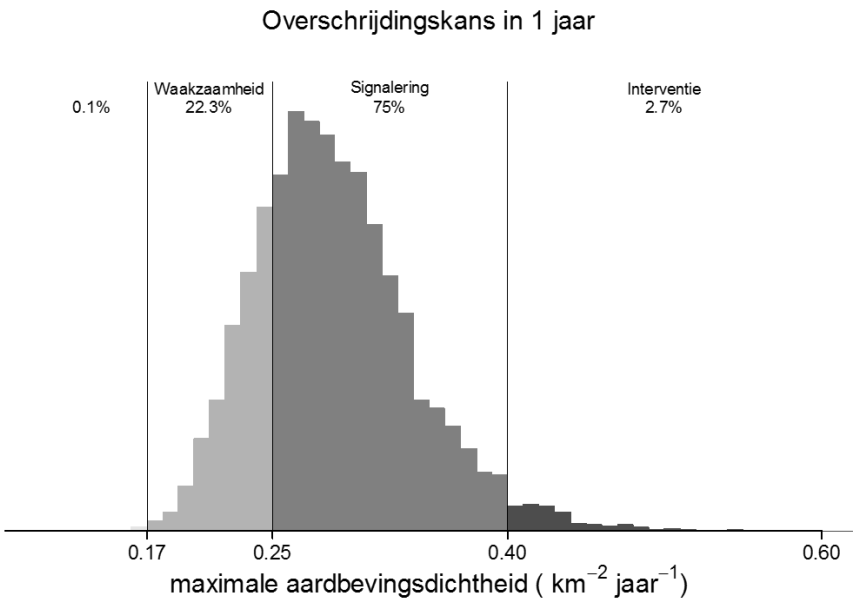

Figure 25 Probability of exceedance (yearly) of the three MRP threshold values.

11 Outline of further work – analysis of individual faults

The last item considered in this report is an outline of work that may make it possible in future to sketch development of seismicity on individual faults (reference 6), where the focus currently is on the predicting seismicity for the full field. Analysis of seismicity developments on individual faults is made possible by two developments:

1. Improved hypocentre location (see also section 7.2)
2. Ongoing geomechanical research

11.1 Progress on hypocentre location and geomechanical research

Interpretation of geophysical data locate seismic events with increasing confidence on known, natural faults. This is enabled by the improved seismic network and better interpretation techniques developed over the recent years, such as full wave inversion and a better velocity model. High-resolution fault interpretation, such as ant-tracking, has been deployed to develop a better geological description of the fault structures in the Groningen field. Furthermore, ongoing experimental work at Utrecht University on the fault and formation properties in the Groningen field has gained insight into the micro- and meso-structural scale of compaction and fault slip. Finally, extensive geomechanical modelling on 3D and 2D scale has been instrumental to gain insight into the conditions under which fault slip and seismic rupture may occur. The developed 2D dynamic rupture simulation capability is able to simulate seismic earthquakes under realistic field conditions and generates wave forms that can be compared with actually observed seismic events.

11.2 Summary of current work

Current efforts are focussing on the integration of these components of the study program in order to better understand individual seismic events, and to develop a relationship between the occurrence of seismicity and the geological setting (offset, fault orientation), the reservoir pressure scenario and underlying geomechanical behaviour of faults. The latter can be expressed by means of a linear slip-weakening diagram (Figure 26). Specifically, calibration of the slope in the slip-weakening diagram W_{μ} is attempted by comparing the wave form data from actual and simulated seismic events (Figure 27).

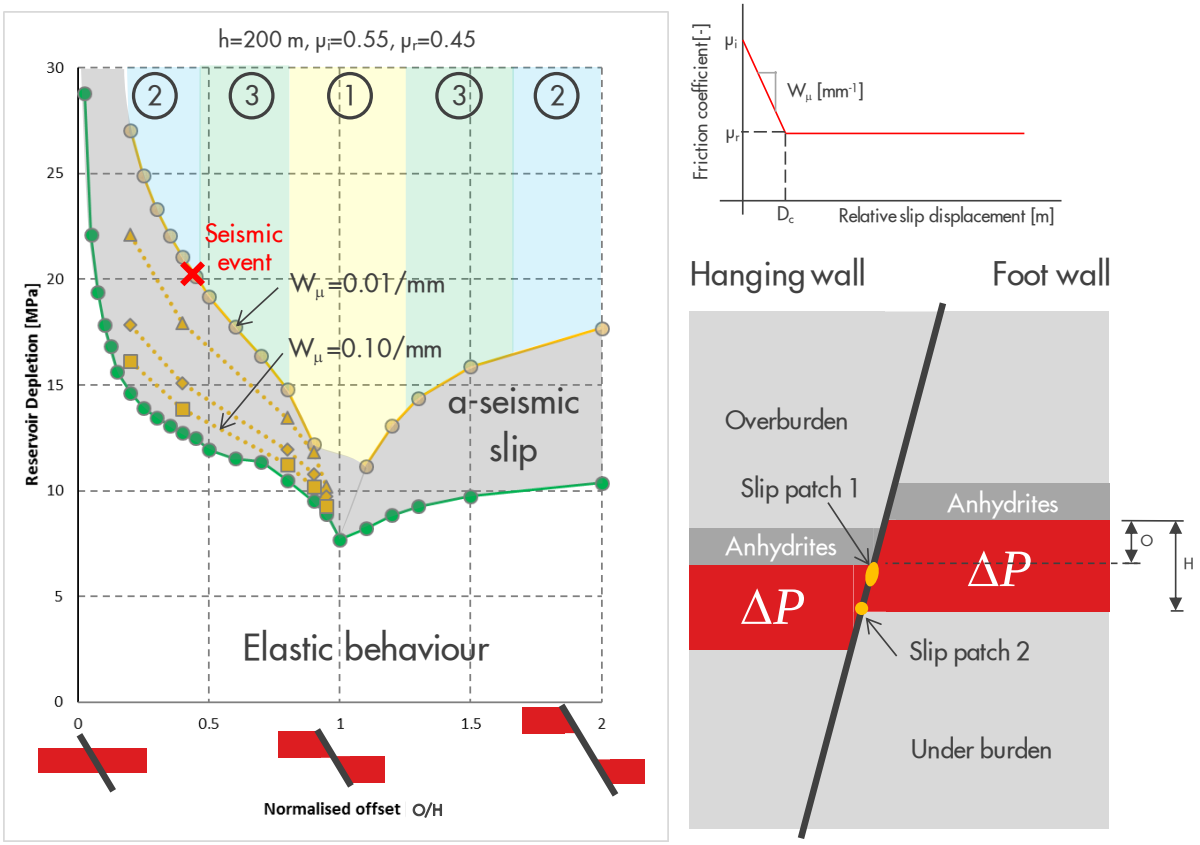

Figure 26 *Bottom-right: Typical Groningen fault configuration with reservoir offset O of about half the reservoir thickness H. A-seismic slip patches occur first at the top of the hanging wall and at the base of the foot wall. Left: The depletion level at which fault slip occurs is strongly dependent on the normalized offset h=O/H as indicated by the green line (right). Seismic rupture occurs (yellow lines) at elevated depletion depending on the slope in the slip-weakening diagram W_μ (top-right).*

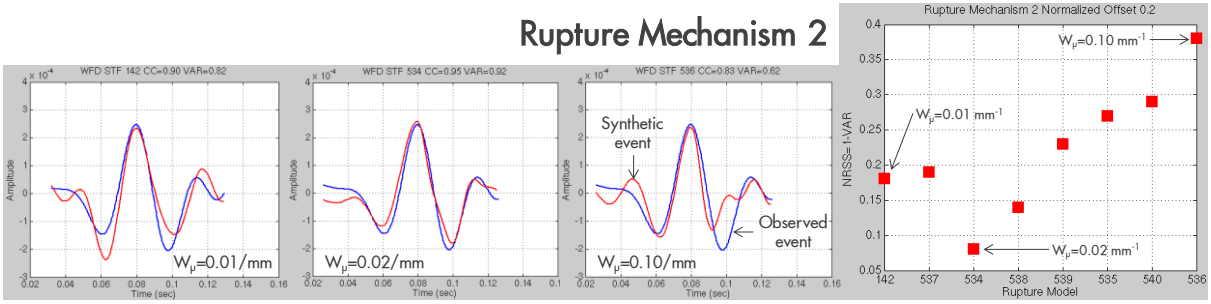

Figure 27 *Comparison of the wave forms from actually observed (blue) and simulated (red) seismic events. The best match (smallest normalised residuals sum of squares, NRSS, right-hand side) with the observed seismic event is obtained for the model with W_μ=0.02 mm^{-1}.*

Successful calibration of the slip-weakening parameter W_μ for an individual or multiple neighbouring seismic events would significantly constrain the three parameters of the linear slip-weakening model. Occurrence of a seismic event would determine a point on the yellow line in Figure 26, based on a known reservoir (depletion) pressure and provided that the normalised reservoir offset can be determined from the geological fault model and the event location. The slope W_μ determines the location of the green line that represents the onset of fault slip, which is determined by the initial friction coefficient μ_i, while the Moment Magnitude determines the reduction of fault strength (μ_i -μ_r). Calibration of the three fault slip parameters μ_i, μ_r and W_μ across the Groningen field would constitute

a step forward in forecasting seismic potential in different parts of the field based on reservoir thickness, offset and fault orientation.

Furthermore, comparison between the wave forms of observed and simulated seismic events may assist in the determination of one of the following three seismic rupture mechanisms:

1. Merging of the two neighbouring a-seismic slip patches
2. Instability of a single slip patch without merging with a neighbouring slip patch
3. Instability of a single slip patch followed by merging with a neighbouring slip patch

The size of the slip patch (Figure 28) could be helpful in understanding the vicinity of multiple seismic events in the same area and the likelihood of merging different seismic and a-seismic slip patches. Merging of slip-weakening parts of a fault constitutes a risk of larger seismic events.

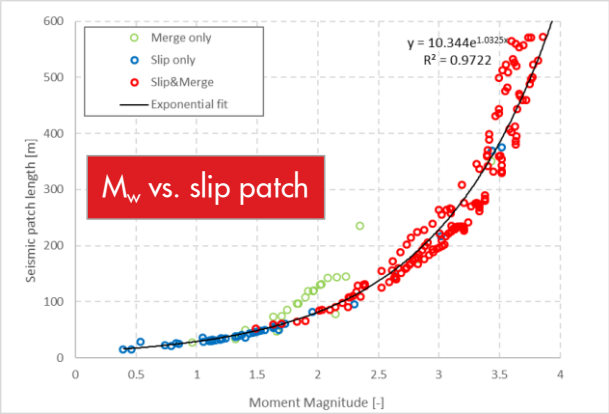

Figure 28 Comparison of the wave forms from actually observed (blue) and simulated (red) seismic events. The best match (smallest normalised residuals sum of squares, NRSS, right-hand side) with the observed seismic event is obtained for the model with W_{μ}=0.02 mm^{-1}.

12 Discussion

Seismicity has been increasing in the Loppersum area during the first half of the year compared to relatively low levels in 2016. This has been highlighted as a concern in earlier reports as well (reference 2). The recent exceedance of the MRP parameter for earthquake density at the signalling level seems to be part of that same development. The two recent earthquakes at ‘t Zandt also triggered a renewed exceedance of the activity rate at the alertness level. No other MRP parameters have been exceeded in the MRP, nor have any concerning patterns or developments been identified in this document. PGV’s and PGA’s associated with these earthquakes were relatively low.

These exceedances have been placed in a historical context and in statistical context arguing that these exceedances are unlikely to be sign of a new worrying pattern, on top of the one already identified (the Q1/Q2 Loppersum increase).

More detailed analysis of the two earthquakes near ‘t Zandt revealed some interesting insights but no worrying signals have been identified. The second earthquake near ‘t Zandt was somewhat associated in time (with a delay of about 2 weeks) with a relative production peak from the ‘t Zandt cluster. The pressure signal associated with this production peak, however, was mild due to diffusion of the signal and it remains hard to imagine that this particular event has been a driving force behind this earthquake. Also, because no consistent association of production peaks with an earthquake could be observed in the field (including ‘t Zandt itself). From a precautionary principle, however, this production procedure (ramp up to 50% of production capacity to clean out the piping) will be reviewed and possibly its frequency can be much reduced.

13 Control Measures

Figure 30 (reproduced from reference 1, the MRP) shows the coupling of measures with exceedances of thresholds of MRP parameters. If no measures would be already in place, the current trend in Loppersum and the exceedance of the earthquake density MRP parameter would have had us to consider control measures ranging from adapting start-up procedures, via closing in a group of clusters to a general reduction of field volumes. It is argued, however, in this report that this exceedance is not part of a new development and that, therefore, the present measure already in place (10% volume reduction per October 2017) should address the underlying cause and some 6-9 months are required to see whether this measure has sufficient an effect. It is proposed to review the situation in June 2018, unless of course new seismic developments require earlier intervention.

Seismicity has been increasing in the Loppersum area during the first half of the year compared to relatively low levels in 2016. This has been highlighted as a concern in earlier reports as well (reference 2). The recent exceedance of the MRP parameter for earthquake density at the signalling level seems to be part of that same development.

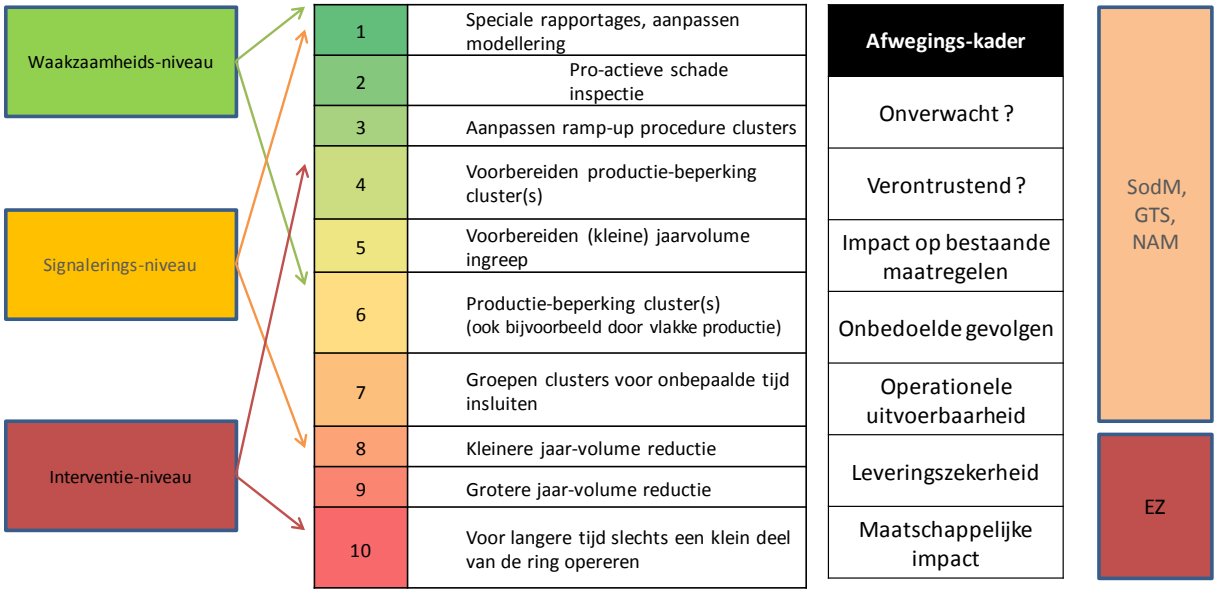

Figure 29 Coupling of control measures to the MRP threshold levels. For detailed description see reference 1.

14 References

1. Measurement and Control Protocol Groningen veld, NAM, June 2017
2. Rapportage Seismiciteit Groningen - 1 november 2017, NAM, November 2017.
3. V5 Ground-Motion Model for the Groningen Field, J.J. Bommer, B. Edwards, P.P. Kruiver, A. Rodriguez-Marek, P.J. Stafford, B. Dost, M. Ntinalexis, E. Ruigrok, J. Spetzler, 30th October 2017.
4. Empirical Ground-Motion Prediction Equations for Peak Ground Velocity from Small-Magnitude Earthquakes in the Groningen Field Using Multiple Definitions of the Horizontal Component of Motion - Updated Model for Application to Smaller Earthquakes, Julian Bommer, Peter Stafford and Michail Ntinalexis, November 2017
5. Groningen Dynamic Model Updates 2017, Van Oeveren, Henk, Valvatne, Per and Geurtsen, Leendert, Assen: NAM, 2017. EP201708205454.
6. Hazard, Building Damage and Risk Assessment, NAM, Jan van Elk and Dirk Doornhof, November 2017